

Multitargeted Imidazoles: Potential Therapeutic Leads for Alzheimer's and Other Neurodegenerative Diseases

Anne-Sophie Cornec,[†] Ludovica Monti,[‡] Jane Kovalevich,[§] Vishruti Makani,[§] Michael J. James,[§] Krishna G. Vijayendran,[†] Killian Oukoloff,[‡] Yuemang Yao,[§] Virginia M.-Y. Lee,[§] John Q. Trojanowski,[§] Amos B. Smith, III,[†] Kurt R. Brunden,^{*,§} and Carlo Ballatore^{*,‡,§}

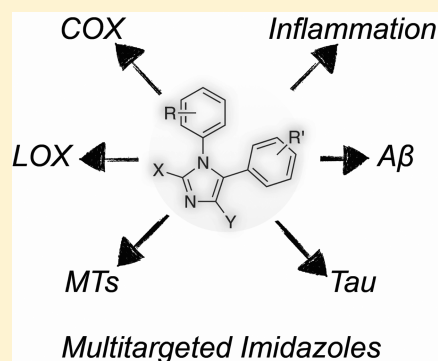
[†]Department of Chemistry, School of Arts and Sciences, University of Pennsylvania, 231 South 34th Street, Philadelphia, Pennsylvania 19104-6323, United States

[‡]Skaggs School of Pharmacy and Pharmaceutical Sciences, University of California, San Diego, 9500 Gilman Drive, La Jolla, California 92093, United States

[§]Center for Neurodegenerative Disease Research, Institute on Aging, University of Pennsylvania, 3600 Spruce Street, Philadelphia, Pennsylvania 19104-6323, United States

Supporting Information

ABSTRACT: Alzheimer's disease (AD) is a complex, multifactorial disease in which different neuropathological mechanisms are likely involved, including those associated with pathological tau and A β species as well as neuroinflammation. In this context, the development of single multitargeted therapeutics directed against two or more disease mechanisms could be advantageous. Starting from a series of 1,5-diarylimidazoles with microtubule (MT)-stabilizing activity and structural similarities with known NSAIDs, we conducted structure–activity relationship studies that led to the identification of multitargeted prototypes with activities as MT-stabilizing agents and/or inhibitors of the cyclooxygenase (COX) and 5-lipoxygenase (5-LOX) pathways. Several examples are brain-penetrant and exhibit balanced multitargeted in vitro activity in the low μ M range. As brain-penetrant MT-stabilizing agents have proven effective against tau-mediated neurodegeneration in animal models, and because COX- and 5-LOX-derived eicosanoids are thought to contribute to A β plaque deposition, these 1,5-diarylimidazoles provide tools to explore novel multitargeted strategies for AD and other neurodegenerative diseases.



INTRODUCTION

In Alzheimer's disease (AD), aggregated tau proteins and A β peptides are thought to participate in disease onset and progression. Moreover, other factors such as neuroinflammation and oxidative stress are also believed to be intimately associated with the neurodegenerative process. Although the precise relationship(s) linking these different neuropathological mechanisms remain the focus of active research, it is clear that AD is a complex and multifactorial disease. Thus far, A β amyloidosis has been the target of choice in AD drug discovery, as most drug candidates have been designed to modulate A β homeostasis. However, in spite of generally strong preclinical data with such therapeutic candidates, the outcomes of late-stage AD clinical trials have thus far failed to demonstrate clinical efficacy. These disappointing results raise the possibility that AD treatments may have to interfere concurrently with more than one neuropathological mechanism to exert disease modifying benefits. In this context, a single multitargeted drug may have distinctive advantages in terms of efficacy and safety over drug combination therapies.¹ As such, an increasing number of therapeutic strategies that are based on polypharmacology have been proposed for AD.^{2,3}

Over the past several years, our laboratories and others have demonstrated that brain-penetrant MT-stabilizing agents have profoundly beneficial effects in animal models of tau pathology due to the ability of these compounds to normalize hyperdynamic axonal MTs, restore axonal transport, reduce the burden of tau pathology, and prevent cognitive impairments and neuron loss associated with tau pathology.^{4–7} Furthermore, our recent work⁸ indicates that the binding of cyclooxygenase (COX)- and 5-lipoxygenase (5-LOX)-derived eicosanoids to their cognate receptors in neurons results in increased production of amyloid precursor protein (APP) and A β peptides, adding to a body of literature^{9–23} implicating inflammatory eicosanoids as key contributing factors to A β plaque deposition in AD. Thus, a stabilization of axonal MTs, combined with a concurrent suppression of eicosanoid production, may be considered as a multitargeted therapeutic strategy that could attenuate both tau- and A β -mediated neurodegeneration, as well as MT deficiencies²⁴ and/or neuroinflammation,^{25–31} in AD. Moreover, this approach may also provide benefit in other neurodegenerative tauopathies.

Received: March 27, 2017

Published: May 22, 2017

The rational design of multitargeted compounds is challenging, especially when attempting to merge multiple molecular frameworks and the corresponding underlying pharmacophores in a single small molecule.³² However, a series of fungicidal diaryl-pyrazoles (e.g., **1**, Figure 1) and -imidazoles (e.g., **2**, Figure 1) with known MT-stabilizing activity exhibit tricyclic structures similar to those found in known nonsteroidal anti-inflammatory drugs (NSAIDs) such as the potent COX-1 inhibitor³³ SC560 (**3**, Figure 1) and, to a lesser extent, the dual COX/5-LOX inhibitor³⁴ licoferone (**4**, Figure 1). Furthermore, molecular docking studies indicated that selected representative examples of these MT-stabilizing imidazoles could fit within the arachidonic acid binding site of COX-1 with a predicted binding energy that is comparable (i.e., within 2 kcal/mol) to that of **3** (see Figure 1 and Supporting Information). Thus, although MT-stabilizing agents and NSAIDs are different classes of biologically active compounds that interact with unrelated targets, the observed structural commonalities between these compounds suggest that there may be significant degree of crosstalk between the different pharmacophores that could be exploited to identify multitargeted ligands. Toward this end, the synthesis and subsequent evaluation of several closely related 1,5-diarylimidazole congeners led to the identification of specific substitution patterns that are required to achieve different activity profiles in vitro. In particular, in addition to identifying compounds that act selectively as MT-stabilizers and others that are selective inhibitors of the COX- and/or 5-LOX pathways with no effect on MTs, these studies led to the identification of a series of multitargeted molecules that at low μM concentration can concurrently stabilize MTs and inhibit both COX- and 5-LOX derived eicosanoids in cell-based assays. Furthermore, several of these compounds were also confirmed to be brain-penetrant, indicating that molecules of this type may be considered as potential multitargeted prototype structures for AD and related tauopathies.

RESULTS

Chemistry. As part of these studies, a library comprising 81 imidazoles has been synthesized, including 36 known compounds (i.e., **2**, **25**, **29–31**, **35**, **36**, **38**, **43–46**, **51**, **54**, **55**, **57**, **58**, **61**, **62**, **64**, **65**, **67**, **68**, **70**, **71**, **73**, **74**, **83–86**, **88**, **92**, **94**, **95**, and **97**, Table 1), most with reported antifungal³⁵ or antimicrobial activity, as well as 45 new structures (i.e., **26–28**, **32–34**, **37**, **39–42**, **47–50**, **52**, **53**, **56**, **59**, **60**, **63**, **66**, **69**, **72**, **75–82**, **87**, **89–91**, **93**, **96**, **98–104**, Table 1). In general, the synthesis of the 1,5-diarylimidazoles was conducted following the Van Leusen imidazole synthesis.³⁶ Thus, after condensation of the appropriate aryl-amine and benzaldehyde, the resulting Schiff base (**5–24**, Scheme 1) was cyclized in the presence of toluenesulfonylmethyl isocyanide (TosMIC) to form the 1,5-diarylimidazole (**25–28**, **32**, **33**, **37–43**, **47–53**, Scheme 1). Further derivatizations of the imidazole ring included the introduction of small alkyl groups and/or halogens in position 2 and/or 4 (**29–31**, **34–36**, and **44–46** in Scheme 1 and **54–104** in Scheme 2). Imidazole derivatives bearing a methyl substituent at C4 were accessed by employing the appropriately C-substituted TosMIC reagent during the cyclization step (**29**, **35**, **44**), while alkylated derivatives at C2 (e.g., **34**, **86**) were obtained by treating the appropriate 1,5-diarylimidazole with LDA followed by addition of the desired alkyl iodide. Finally, halogenation of the imidazole ring was accomplished upon treatment with *N*-chlorosuccinimide. When the halogenation was carried out on imidazoles that were not substituted at C2 and C4, the reaction typically proceeded with the generation of separable mixtures of mono- and dichlorinated imidazoles.

Structure–Activity Relationships. The MT-stabilizing activity of test compounds was determined in QBI-293 cells by monitoring compound-induced elevation in acetylated α -tubulin (AcTub),³⁷ which is a known marker of stable MTs.³⁸ Furthermore, as the MT-stabilizing imidazoles are believed to act on MTs in a manner similar to that described for the triazolopyrimidines,³⁵ and considering that certain triazolopyr-

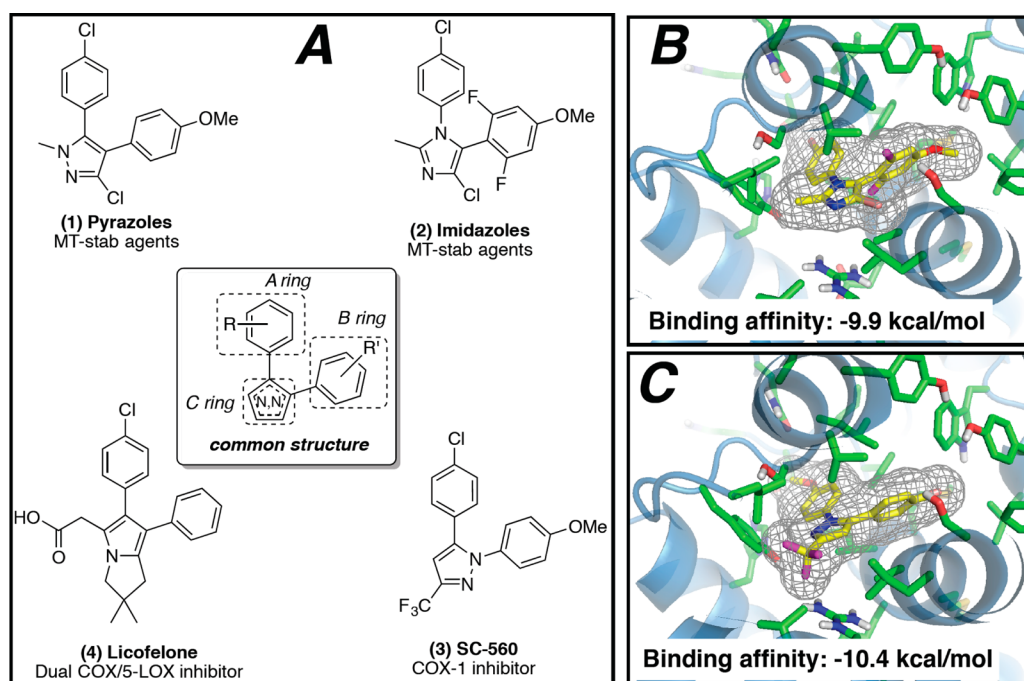


Figure 1. (A) Comparison of representative examples of fungicidal diaryl-pyrazoles (**1**) and -imidazoles (**2**) with reported MT-stabilizing activity, with known COX- (**3**) and dual COX/5-LOX (**4**) inhibitors; molecular docking of **2** (B) and **3** (C) within the arachidonic acid binding site of COX-1.

Scheme 1^a

A = 4-chlorophenyl; **B** = 2,4,6-trifluorophenyl (**5**)
A = 4-methoxyphenyl; **B** = 2,4,6-trifluorophenyl (**6**)
A = 4-chlorophenyl; **B** = 2,6-difluoro-3-methylphenyl (**7**)
A = 4-chlorophenyl; **B** = 3-chloro-2,6-difluorophenyl (**8**)
A = 4-chlorophenyl; **B** = 3-bromo-2,6-difluorophenyl (**9**)
A = 4-chlorophenyl; **B** = 2,3,6-trifluorophenyl (**10**)
A = 4-chloro-3-fluorophenyl; **B** = 2,3,6-trifluorophenyl (**11**)
A = 6-chloropyridin-3-yl; **B** = 2,4,6-trifluorophenyl (**12**)
A = 4-chlorophenyl; **B** = 4-fluorophenyl (**13**)
A = 4-chloro-2-fluorophenyl; **B** = 2,6-difluorophenyl (**14**)
A = 4-chlorophenyl; **B** = 2,5-difluorophenyl (**15**)
A = 4-(trifluoromethoxy)phenyl; **B** = 2,6-difluorophenyl (**16**)
A = 4-chlorophenyl; **B** = 2,6-difluorophenyl (**17**)
A = 4-(trifluoromethoxy)phenyl; **B** = 2,3,6-trifluorophenyl (**18**)
A = 4-chlorophenyl; **B** = 2,6-difluoro-4-methylphenyl (**19**)
A = 4-chlorophenyl; **B** = 2,6-difluoro-3-methoxyphenyl (**20**)
A = 4-chlorophenyl; **B** = phenyl (**21**)
A = 4-chlorophenyl; **B** = 4-methoxyphenyl (**22**)
A = phenyl; **B** = 2,6-difluorophenyl (**23**)
A = 2-chlorophenyl; **B** = 2,6-difluorophenyl (**24**)

X = H; **Y** = H; **A** = 4-chlorophenyl; **B** = 2,4,6-trifluorophenyl (**25**)
X = H; **Y** = H; **A** = 4-methoxyphenyl; **B** = 2,4,6-trifluorophenyl (**26**)
X = H; **Y** = H; **A** = 4-chlorophenyl; **B** = 2,6-difluoro-3-methylphenyl (**27**)
X = H; **Y** = H; **A** = 4-chlorophenyl; **B** = 3-chloro-2,6-difluorophenyl (**28**)
X = H; **Y** = Me; **A** = 4-chlorophenyl; **B** = 3-chloro-2,6-difluorophenyl (**29**)
X = Cl; **Y** = Me; **A** = 4-chlorophenyl; **B** = 3-chloro-2,6-difluorophenyl (**30**) $\leftarrow d$
X = Me; **Y** = Me; **A** = 4-chlorophenyl; **B** = 3-chloro-2,6-difluorophenyl (**31**) $\leftarrow e$
X = H; **Y** = H; **A** = 4-chlorophenyl; **B** = 3-bromo-2,6-difluorophenyl (**32**)
X = H; **Y** = H; **A** = 4-chlorophenyl; **B** = 2,3,6-trifluorophenyl (**33**) $\leftarrow e$
X = Me; **Y** = H; **A** = 4-chlorophenyl; **B** = 2,3,6-trifluorophenyl (**34**) $\leftarrow e$
X = H; **Y** = Me; **A** = 4-chlorophenyl; **B** = 2,3,6-trifluorophenyl (**35**) $\leftarrow d$
X = Cl; **Y** = Me; **A** = 4-chlorophenyl; **B** = 2,3,6-trifluorophenyl (**36**) $\leftarrow d$
X = H; **Y** = H; **A** = 4-chloro-3-fluorophenyl; **B** = 2,3,6-trifluorophenyl (**37**)
X = H; **Y** = H; **A** = 6-chloropyridin-3-yl; **B** = 2,4,6-trifluorophenyl (**38**)
X = H; **Y** = H; **A** = 4-chlorophenyl; **B** = 4-fluorophenyl (**39**)
X = H; **Y** = H; **A** = 4-chloro-2-fluorophenyl; **B** = 2,6-difluorophenyl (**40**)
X = H; **Y** = H; **A** = 4-chlorophenyl; **B** = 2,5-difluorophenyl (**41**)
X = H; **Y** = H; **A** = 4-(trifluoromethoxy)phenyl; **B** = 2,6-difluorophenyl (**42**)
X = H; **Y** = H; **A** = 4-chlorophenyl; **B** = 2,6-difluorophenyl (**43**)
X = H; **Y** = Me; **A** = 4-chlorophenyl; **B** = 2,6-difluorophenyl (**44**) $\leftarrow d$
X = Cl; **Y** = Me; **A** = 4-chlorophenyl; **B** = 2,6-difluorophenyl (**45**) $\leftarrow e$
X = Me; **Y** = Me; **A** = 4-chlorophenyl; **B** = 2,6-difluorophenyl (**46**) $\leftarrow e$
X = H; **Y** = H; **A** = 4-(trifluoromethoxy)phenyl; **B** = 2,3,6-trifluorophenyl (**47**)
X = H; **Y** = H; **A** = 4-chlorophenyl; **B** = 2,6-difluoro-4-methylphenyl (**48**)
X = H; **Y** = H; **A** = 4-chlorophenyl; **B** = 2,6-difluoro-3-methoxyphenyl (**49**)
X = H; **Y** = H; **A** = 4-chlorophenyl; **B** = phenyl (**50**)
X = H; **Y** = H; **A** = 4-chlorophenyl; **B** = 4-methoxyphenyl (**51**)
X = H; **Y** = H; **A** = phenyl; **B** = 2,6-difluorophenyl (**52**)
X = H; **Y** = H; **A** = 2-chlorophenyl; **B** = 2,6-difluorophenyl (**53**)

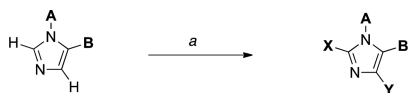
^aReagents and reaction conditions: (a) Dean–Stark apparatus, toluene, 110 °C, 4 days, 99%; (b) 4 Å molecular sieves, Et₂O, 30 °C, 48 h, 99%; (c) appropriate TosMIC reagent, K₂CO₃, DMF/1,2-dimethoxyethane, 100 °C, 16 h, 7–90%; (d) *N*-chlorosuccinimide, CHCl₃, 60 °C, 16 h, 43–71%; (e) LDA, methyl iodide, THF, –20 °C to rt, 1.5 h, 29–56%.

imidines have been found to induce a proteasome-dependent degradation of α -tubulin,³⁹ the effect of compound treatment on total α -tubulin was also monitored. Evaluation of compound inhibition of the biosynthesis of COX- and 5-LOX-derived eicosanoids was conducted in a modified rat basophilic leukemia (RBL-1) cell assay that has previously been described⁴⁰ for the evaluation of 5-LOX and which we found can be used to assess both COX-derived prostaglandins (PGs) and 5-LOX-derived leukotrienes (LTs) formed in the presence or absence of test compounds.

All compounds were initially screened at 1 and 10 μ M concentration in the QBI cell MT assay and at 10 μ M in the RBL-1 cell assay (Table 1). In this initial RBL-1 cell analysis, 5-LOX-derived LTB₄ and COX-derived PGD₂ and PGE₂, which coeluted during LC/MS/MS, were quantified. Selected compounds (Table 2) exhibiting evidence of multitargeted activity underwent further confirmatory studies in the RBL-1 cell assay, which included concentration–response testing, and further LC/MS/MS analyses using a refined protocol to individually detect and quantitate PGD₂ and PGE₂, as well as both LTB₄ and LTC₄. As the formation of each of these eicosanoids depends on separate enzymatic steps in the COX or 5-LOX pathways,⁴¹ concurrent analysis of all four of these eicosanoids provides a convenient and reliable method to evaluate the overall effect of test compounds on COX and 5-LOX pathways in a cellular milieu. Finally, several compounds in Table 2 were also assessed for their relative brain-to-plasma exposure levels after administration to mice.

MT-Stabilizing Activity. Evaluation of compounds in the QBI-293 cell MT assay revealed that out of 71 tested compounds,

48 examples exhibited activity on MTs as revealed by statistically significant changes in AcTub levels. Among MT-active compounds, seven examples (i.e., **2**, **58**, **65**, **71**, **85**, **86**, and **97**) were found to be active at 1 μ M compound concentration, whereas the remaining 41 compounds were active only at 10 μ M. Consistent with the notion that the MT-stabilizing 1,5-diarylimidazoles may be acting on MTs in a similar manner as the triazolopyrimidines,³⁵ the data presented in Table 1 reveal that like the latter molecules, these imidazoles can be broadly divided into two subsets: one group of 15 entries, which cause a significant reduction in total α -tubulin levels at doses typically required to induce an elevation in AcTub (i.e., **2**, **30**, **34**, **58**, **62**, **63**, **65**, **66**, **71**, **73**, **85**, **94**–**97**) and a second group of 33 compounds that produce an elevation in AcTub at 1 or 10 μ M without decreasing α -tubulin level (**29**, **31**, **35**, **36**, **44**–**46**, **54**, **55**–**57**, **59**, **60**, **64**, **67**–**70**, **72**, **74**, **78**, **82**–**84**, **86**–**88**, **90**–**93**, **102**, **104**). Also of interest, a comparison of the activities of compounds in the AcTub assay at 1 and 10 μ M suggest that selected entries, such as compounds **2**, **58**, and **71**, may exhibit a bell-shaped concentration–response relationship, and it is possible that additional examples would show a similar concentration–response if tested at higher concentrations. This phenomenon was observed in the case of the triazolopyrimidines that reduce α -tubulin level, such as **108**.³⁹ Irrespective of whether or not test compounds cause a reduction in total α -tubulin, the AcTub SAR emerging from the data shown in Table 1 appear to be in general agreement with SAR from prior studies in which MT-stabilizing 1,5-diarylimidazoles were evaluated for antifungal activity.³⁵ Thus, our results indicate that ring A is preferably a 4-chloro-

Scheme 2^a

- X = H; Y = Cl; A = 4-chlorophenyl; B = 2,4,6-trifluorophenyl (54) ← b
 X = Me; Y = Cl; A = 4-chlorophenyl; B = 2,4,6-trifluorophenyl (55) ← b
 X = Me; Y = Cl; A = 4-chlorophenyl; B = 2,6-difluoro-4-methoxyphenyl (2) ← c
 X = Cl; Y = H; A = 4-chlorophenyl; B = 2,4,6-trifluorophenyl (56)
 X = Cl; Y = Cl; A = 4-chlorophenyl; B = 2,4,6-trifluorophenyl (57)
 X = Cl; Y = Cl; A = 4-chlorophenyl; B = 2,6-difluoro-4-methoxyphenyl (58) ← c
 X = H; Y = Cl; A = 4-methoxyphenyl; B = 2,4,6-trifluorophenyl (59)
 X = Cl; Y = H; A = 4-methoxyphenyl; B = 2,4,6-trifluorophenyl (60)
 X = Cl; Y = Cl; A = 4-methoxyphenyl; B = 2,4,6-trifluorophenyl (61)
 X = H; Y = Cl; A = 4-chlorophenyl; B = 2,6-difluoro-3-methylphenyl (62)
 X = Cl; Y = H; A = 4-chlorophenyl; B = 2,6-difluoro-3-methylphenyl (63)
 X = H; Y = Cl; A = 4-chlorophenyl; B = 3-chloro-2,6-difluorophenyl (64)
 X = Me; Y = Cl; A = 4-chlorophenyl; B = 3-chloro-2,6-difluorophenyl (65) ← b
 X = Cl; Y = H; A = 4-chlorophenyl; B = 3-chloro-2,6-difluorophenyl (66)
 X = H; Y = Cl; A = 4-chlorophenyl; B = 3-bromo-2,6-difluorophenyl (67)
 X = H; Y = Cl; A = 4-chlorophenyl; B = 2,3,6-trifluorophenyl (68)
 X = Cl; Y = H; A = 4-chlorophenyl; B = 2,3,6-trifluorophenyl (69)
 X = H; Y = Cl; A = 4-chloro-3-fluorophenyl; B = 2,3,6-trifluorophenyl (70) ← b
 X = Me; Y = Cl; A = 4-chloro-3-fluorophenyl; B = 2,3,6-trifluorophenyl (71) ← b
 X = Cl; Y = H; A = 4-chloro-3-fluorophenyl; B = 2,3,6-trifluorophenyl (72)
 X = H; Y = Cl; A = 6-chloropyridin-3-yl; B = 2,4,6-trifluorophenyl (73) ← b
 X = Me; Y = Cl; A = 6-chloropyridin-3-yl; B = 2,4,6-trifluorophenyl (74) ← b
 X = Cl; Y = H; A = 4-chlorophenyl; B = 4-fluorophenyl (75)
 X = H; Y = Cl; A = 4-chlorophenyl; B = 4-fluorophenyl (76)
 X = Cl; Y = H; A = 4-chloro-2-fluorophenyl; B = 2,6-difluorophenyl (77)
 X = H; Y = Cl; A = 4-chloro-2-fluorophenyl; B = 2,6-difluorophenyl (78)
 X = Cl; Y = H; A = 4-chlorophenyl; B = 2,5-difluorophenyl (79)
 X = H; Y = Cl; A = 4-chlorophenyl; B = 2,5-difluorophenyl (80)
 X = H; Y = Cl; A = 4-(trifluoromethoxy)phenyl; B = 2,6-difluorophenyl (81)
 X = Cl; Y = H; A = 4-(trifluoromethoxy)phenyl; B = 2,6-difluorophenyl (82)
 X = Cl; Y = Cl; A = 4-(trifluoromethoxy)phenyl; B = 2,6-difluorophenyl (83)
 X = H; Y = Cl; A = 4-chlorophenyl; B = 2,6-difluorophenyl (84) ← b
 X = Me; Y = Cl; A = 4-chlorophenyl; B = 2,6-difluorophenyl (85) ← b
 X = Et; Y = Cl; A = 4-chlorophenyl; B = 2,6-difluorophenyl (86) ← d
 X = Cl; Y = H; A = 4-chlorophenyl; B = 2,6-difluorophenyl (87)
 X = Cl; Y = Cl; A = 4-chlorophenyl; B = 2,6-difluorophenyl (88)
 X = H; Y = Cl; A = 4-(trifluoromethoxy)phenyl; B = 2,3,6-trifluorophenyl (89)
 X = Cl; Y = H; A = 4-(trifluoromethoxy)phenyl; B = 2,3,6-trifluorophenyl (90)
 X = Cl; Y = Cl; A = 4-(trifluoromethoxy)phenyl; B = 2,3,6-trifluorophenyl (91)
 X = H; Y = Cl; A = 4-chlorophenyl; B = 2,6-difluoro-4-methylphenyl (92)
 X = Cl; Y = H; A = 4-chlorophenyl; B = 2,6-difluoro-4-methylphenyl (93)
 X = Cl; Y = Cl; A = 4-chlorophenyl; B = 2,6-difluoro-4-methylphenyl (94)
 X = H; Y = Cl; A = 4-chlorophenyl; B = 2,6-difluoro-3-methoxyphenyl (95)
 X = Cl; Y = H; A = 4-chlorophenyl; B = 2,6-difluoro-3-methoxyphenyl (96)
 X = Cl; Y = Cl; A = 4-chlorophenyl; B = 2,6-difluoro-3-methoxyphenyl (97)
 X = H; Y = Cl; A = 4-chlorophenyl; B = phenyl (98)
 X = Cl; Y = H; A = 4-chlorophenyl; B = phenyl (99)
 X = Cl; Y = Cl; A = 4-chlorophenyl; B = phenyl (100)
 X = H; Y = Cl; A = 4-chlorophenyl; B = 4-methoxyphenyl (101)
 X = H; Y = Cl; A = 2-chlorophenyl; B = 2,6-difluorophenyl (102)
 X = Cl; Y = H; A = 2-chlorophenyl; B = 2,6-difluorophenyl (103)
 X = Cl; Y = Cl; A = 2-chlorophenyl; B = 2,6-difluorophenyl (104) ← a

^aReagents and reaction conditions: (a) *N*-chlorosuccinimide, CHCl₃, 60 °C, 16 h, 9–77% for monohalogenation at C4, 3–18% for monohalogenation at C2, and 2–20% for dihalogenation at C2/C4; (b) LDA, methyl iodide, THF, –20 °C to rt, 1.5 h, 2–48%; (c) NaOMe, MeOH, THF, rt, 19 h, 33–97%; (d) LDA, ethyl iodide, THF, –20 °C to rt, 1.5 h, 35%.

phenyl, although examples bearing other substituents in the *para*-position, such as a trifluoromethoxy (83), are also active. Additional substitutions in the A ring, as in compound 77 and 78 in which a fluorine is present in the *ortho*-position, appear to impact negatively MT interactions of the compound (cf. 77 with 87 and 78 with 84). With respect to the B ring, the degree and pattern of fluorination appear to be generally important factors that determine the ability of these imidazoles to produce a significant elevation in the marker of stable MTs in QBI-293 cells. Whereas derivatives with either one or no fluorination in the B ring (i.e., 50, 51, 75, 76, 98–101) were found to be essentially devoid of MT activity in our assay conditions, other di- and trisubstituted congeners (e.g., 54, 68, 84) produced a significant increase in AcTub. Furthermore, a comparison between the inactive difluorinated derivative 80 and the active di- and trifluorinated compounds (i.e., 54, 68, and 84) suggests

that the presence of two fluorine atoms in the *ortho*-positions of ring B is required for MT activity. Finally, with respect to the imidazole ring (ring C), our results indicate that 1,5-diarylimidazoles that are not substituted in positions 2 and 4 (e.g., 25, 26, 42, 43, 48, 49, 52, and 53) do not cause a detectable increase in AcTub, whereas tetrasubstituted imidazoles, including C2/C4 dihalogenated (e.g., 88) and dimethylated (e.g., 46) derivatives, as well as analogues bearing both a small alkyl- and a chloro-substituent in either C2 or C4 positions (e.g., 85 and 45), are generally more active than corresponding derivatives bearing a single substitution in either position 2 or 4 (cf. 87, 88, and 44, 46). These results also suggest that MT activity does not strictly require a halogen in position 4 of the imidazole ring, as was required for optimal antifungal activity,³⁵ because congeners halogenated at C2 appear to retain comparable MT activity (cf. 54, 56 and 84, 87).

Inhibition of Prostaglandin Biosynthetic Pathway.

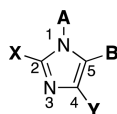
Evaluation of test compounds as potential inhibitors of COX-dependent formation of PGD₂/PGE₂ in RBL-1 cells revealed that optimal inhibition of PG synthesis is typically achieved when ring A is substituted in the *para*-position with either a chloride (e.g., 54) or methoxy group (e.g., 59). With respect to ring B, comparison of 54, 68, 76, 79, 84, and 98 clearly suggests that the presence of fluorine substituents is not detrimental, or necessary, for inhibition of PG production. Evaluation of the effect of different substitutions in the imidazole ring reveals that, with the possible exception of compound 104, which shows a >50% inhibition in the PGD₂/PGE₂ assay, tetrasubstituted compounds (e.g., 45, 46, 85, 88) are generally devoid of inhibitory activity against PG synthesis. Conversely, 1,5-diarylimidazole congeners with one substitution at either C2 or C4 are generally active, with the presence of a substituent at C4 being possibly preferred over the C2 position (cf. 62 with 63, 64 with 66, 84 with 87, and 92 with 93). Among 1,5-diarylimidazoles that are not substituted at C2 and C4, although these compounds appear to be generally less active than the corresponding compounds bearing a substituent at C2 or C4, selected examples, such as 51, have been identified that produce a near complete inhibition of the combined PGD₂/PGE₂ synthesis in the RBL-1 cell assay when tested at 10 μM.

Inhibition of Leukotriene Biosynthetic Pathway.

Finally, evaluation of compound inhibitory activity in the LTB₄ assay revealed that whereas a number of substitutions in the *para*-position of ring A appeared to be well tolerated, the presence of a 2-chloro-pyridine (see 73 and 74) prevented inhibition of LTB₄ synthesis. In addition, similarly to what was observed for the SAR of PGD₂/PGE₂ synthesis inhibition, the fluorination of the B ring did not impact activity, as both fluorinated (e.g., 59, 80 and 84) and nonfluorinated (e.g., 98) congeners exhibit comparable inhibitory activity in the LTB₄ assay. However, in contrast to what was observed for inhibitory activity against PG synthesis, the choice of substituents at C2 and/or C4 of the imidazole ring did not play a critical role as examples of di- (e.g., 47), tri- (e.g., 89 and 90) and tetra-substituted (e.g., 91) imidazoles were found to exhibit comparable suppression of LTB₄ synthesis in RBL-1 cells at 10 μM.

Thus, in light of the observed elements of SAR for the three biological targets, the particular substitution pattern decorating the 1,5-diarylimidazole scaffold can result in compounds with different activity profiles, including multitargeted activity on MTs and/or eicosanoid biosynthesis (Figure 2). Selected representative examples of multitargeted compounds were

Table 1. Evaluation of Test Compounds as MT-Stabilizing Agents and Inhibitors of COX- and 5-LOX Pathways



Cpd #	X	Y	Ring A	Ring B	PGD ₂ /E ₂ % Inhibition at 10 μM ^a	LTB ₄ % Inhibition at 10 μM ^b	Relative Change in AcTub ^c	Relative Change in α-Tubulin ^d
2	Me	Cl			39	88	× 7.1 (1 μM)** × 2.9 (10 μM)**	× 0.6 (1 μM)** × 0.3 (10 μM)**
25	H	H			44	24	NS	NS
26	H	H			65	25	NS	NS
29	H	Me			59	71	× 3.5 (10 μM)**	NS
30	Cl	Me			<10	54	× 9.2 (10 μM)**	× 0.5 (10 μM)**
31	Me	Me			<10	51	× 14.2 (10 μM)**	NS
34	Me	H			49	45	× 4.7 (10 μM)**	× 0.9 (10 μM)**
35	H	Me			74	74	× 3.4 (10 μM)**	× 1.2 (1 μM)**
36	Cl	Me			<10	58	× 14.3 (10 μM)**	NS
42	H	H			38	55	NS	NS
43	H	H			15	46	NS	× 1.2 (1 μM)*
44	H	Me			72	44	× 1.6 (10 μM)**	NS
45	Cl	Me			<10	42	× 4.1 (10 μM)**	NS
46	Me	Me			<10	40	× 8.3 (10 μM)**	× 1.2 (1 μM)*

Table 1. continued

Cpd #	X	Y	Ring A	Ring B	PGD ₂ /E ₂ % Inhibition at 10 μM ^a	LTB ₄ % Inhibition at 10 μM ^b	Relative Change in AcTub ^c	Relative Change in α- Tubulin ^d
47	H	H			31	52	NS	× 1.2 (10 μM)*
48	H	H			66	84	NS	NS
49	H	H			<10	78	NS	NS
50	H	H			40	16	NS	NS
51	H	H			94	<10	NS	NS
52	H	H			19	<10	NS	NS
53	H	H			24	<10	NS	NS
54	H	Cl			91	46	× 3.3 (10 μM)**	NS
55	Me	Cl			<10	<10	× 5.7 (10 μM)**	NS
56	Cl	H			34	61	× 3.1 (10 μM)**	NS
57	Cl	Cl			<10	48	× 4.2 (10 μM)**	NS
58	Cl	Cl			12	38	× 3.3 (1 μM)** × 2.5 (10 μM)**	× 0.6 (1 μM)** × 0.3 (10 μM)**
59	H	Cl			93	86	× 4.1 (10 μM)**	NS
60	Cl	H			85	75	× 3.4 (10 μM)**	NS
62	H	Cl			79	78	× 2.2 (10 μM)**	× 0.8 (10 μM)**
63	Cl	H			<10	69	× 2.3 (10 μM)**	× 0.8 (1 μM)** × 0.9 (10 μM)**

Table 1. continued

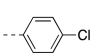
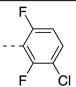
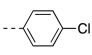
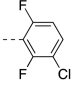
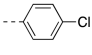
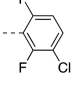
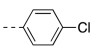
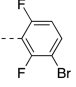
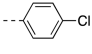
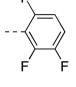
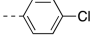
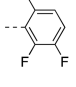
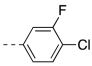
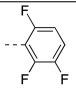
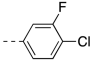
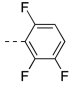
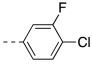
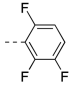
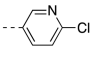
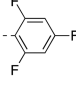
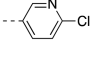
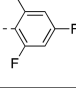

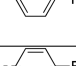
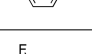
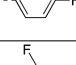
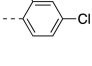
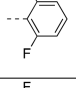
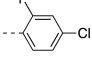
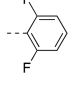
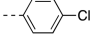
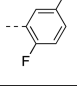
Cpd #	X	Y	Ring A	Ring B	PGD ₂ /E ₂ % Inhibition at 10 μM ^a	LTB ₄ % Inhibition at 10 μM ^b	Relative Change in AcTub ^c	Relative Change in α- Tubulin ^d
64	H	Cl			71	63	× 2.4 (10 μM)**	NS
65	Me	Cl			34	84	× 1.7 (1 μM)** × 9.7 (10 μM)**	× 0.6 (10 μM)**
66	Cl	H			<10	88	× 2.2 (10 μM)**	× 0.8 (10 μM)**
67	H	Cl			54	78	× 2.1 (10 μM)**	NS
68	H	Cl			82	69	× 2.0 (10 μM)**	NS
69	Cl	H			26	24	× 2.4 (10 μM)**	NS
70	H	Cl			74	66	× 1.9 (10 μM)**	NS
71	Me	Cl			<10	75	× 3.9 (1 μM)** × 2.4 (10 μM)**	× 0.8 (1 μM)** × 0.7 (10 μM)**
72	Cl	H			32	58	× 3.2 (10 μM)**	NS
73	H	Cl			65	<10	× 1.9 (10 μM)**	× 0.8 (10 μM)**
74	Me	Cl			<10	26	× 4.4 (10 μM)**	NS
75	Cl	H			87	57	NS	NS
76	H	Cl			85	59	NS	NS
77	Cl	H			<10	49	NS	NS
78	H	Cl			36	14	× 2.6 (10 μM)**	NS
79	Cl	H			76	96	NS	NS

Table 1. continued

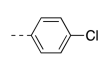
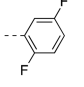
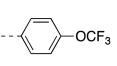
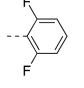
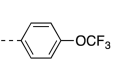
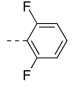
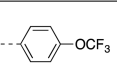
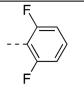
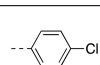
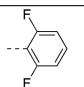
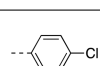
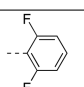
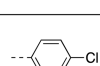
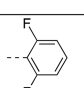
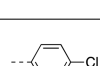
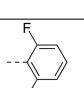
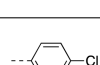
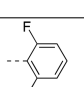
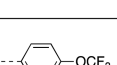
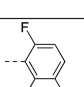
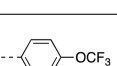
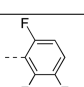
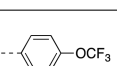
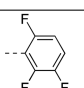
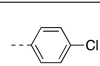
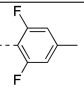
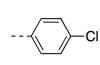
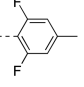
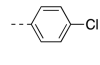
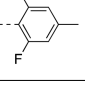
Cpd #	X	Y	Ring A	Ring B	PGD ₂ /E ₂ % Inhibition at 10 μM ^a	LTB ₄ % Inhibition at 10 μM ^b	Relative Change in AcTub ^c	Relative Change in α- Tubulin ^d
80	H	Cl			46	69	NS	NS
81	H	Cl			46	78	NS	NS
82	Cl	H			19	61	× 2.2 (10 μM)**	NS
83	Cl	Cl			19	81	× 6.1 (10 μM)**	NS
84	H	Cl			94	76	× 4.0 (10 μM)**	NS
85	Me	Cl			45	87	× 2.5 (1 μM)* × 15.7 (10 μM)**	× 0.8 (10 μM)**
86	Et	Cl			30	81	× 1.8 (1 μM)** × 5.0 (10 μM)**	NS
87	Cl	H			50	92	× 4.8 (10 μM)**	NS
88	Cl	Cl			17	90	× 7.7 (10 μM)**	NS
89	H	Cl			54	85	NS	NS
90	Cl	H			58	80	× 3.4 (10 μM)**	NS
91	Cl	Cl			40	56	× 6.3 (10 μM)**	NS
92	H	Cl			90	75	× 3.6 (10 μM)**	NS
93	Cl	H			42	73	× 5.7 (10 μM)**	NS
94	Cl	Cl			<10	63	× 18.2 (10 μM)**	× 0.7 (10 μM)**

Table 1. continued

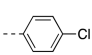
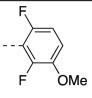
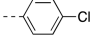
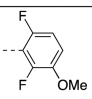
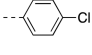
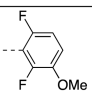
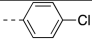
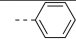
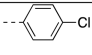
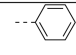
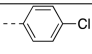
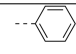
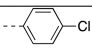
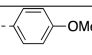
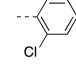
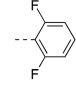
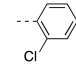
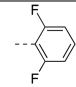
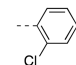
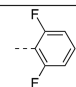
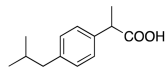
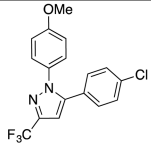
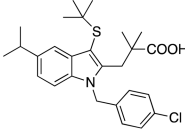
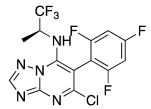
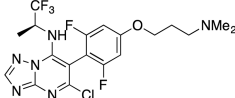
Cpd #	X	Y	Ring A	Ring B	PGD ₂ /E ₂ % Inhibition at 10 μM ^a	LTB ₄ % Inhibition at 10 μM ^b	Relative Change in AcTub ^c	Relative Change in α-Tubulin ^d
95	H	Cl			48	91	× 4.0 (10 μM)**	× 0.8 (10 μM)**
96	Cl	H			<10	68	× 8.2 (10 μM)**	× 0.6 (10 μM)**
97	Cl	Cl			17	88	× 5.1 (1 μM)** × 10.1 (10 μM)**	× 0.9 (1 μM)** × 0.4 (10 μM)**
98	H	Cl			94	71	NS	NS
99	Cl	H			75	52	NS	× 1.2 (10 μM)**
100	Cl	Cl			14	<10	NS	NS
101	H	Cl			95	<10	NS	NS
102	H	Cl			44	56	× 3.5 (10 μM)**	NS
103	Cl	H			28	38	NS	NS
104	Cl	Cl			66	21	× 3.8 (10 μM)**	NS
Ibuprofen (105)					95	<10	NS	NS
3					79 [§]	<10 [§]	NS	NS
MK866 (106) ⁴²					<10 [§]	70 [§]	ND	ND
Triazolopyrimidine (107)					ND	ND	× 2.5 (1 μM) [^] , × 4.9 (10 μM) [^]	NS

Table 1. continued

Cpd #	X	Y	Ring A	Ring B	PGD ₂ /E ₂ % Inhibition at 10 μM ^a	LTB ₄ % Inhibition at 10 μM ^b	Relative Change in AcTub ^c	Relative Change in α-Tubulin ^d
Triazolopyrimidine (108)					ND	ND	× 6.0 (1 μM) [^] , × 0.5 (10 μM) [^]	× 0.7 (1 μM), × 0.4 (10 μM)

^aInhibition of COX pathway was determined by monitoring via LC/MS/MS analyses the combined production of COX-derived PGD₂ and PGE₂ in RBL-1 cells upon stimulation with arachidonic acid in the presence or absence of test compounds, with all samples run in at least triplicate.

^bInhibition of 5-LOX pathway was determined by monitoring via LC/MS/MS analyses the production of 5-LOX-derived LTB₄ in RBL-1 cells upon stimulation with arachidonic acid in the presence or absence of test compounds, with all samples run in at least triplicate. ^cMT-stabilizing activity in QBI-293 cells was determined by monitoring via ELISA the changes in acetylated α-tubulin levels relative to vehicle treatment in response to 4 h treatment with 1 and 10 μM test compounds, with all samples run in at least triplicate. The compound concentrations causing a significant change in AcTub are listed, along with the fold-change in AcTub. ^dRelative changes in total α-tubulin, as determined by tubulin ELISA, in response to 1 and 10 μM compound treatment, with all samples run in at least triplicate. The compound concentrations causing a significant change in α-Tub are listed, along with the fold-change in α-Tub. [^], Compound tested at 10 nM. [^], Previously published data.³⁹ *, P < 0.05. **, P < 0.01 compared with vehicle (DMSO)-treated controls as determined using a two-tailed unpaired *t* test. NS, not significant. ND, not determined.

evaluated further to determine the IC₅₀ values in the RBL-1 cell assays and brain penetration (see Figure 3 and Table 2). Moreover, the compounds in Table 2 were also examined with improved LC/MS/MS methodologies for their ability to inhibit the individual COX-derived products PGE₂ and PGD₂ as well as a second 5-LOX-derived product, LTC₄ (see Supporting Information, Figure S1). Finally, two example compounds underwent full concentration–response analyses in the AcTub assay (see Supporting Information, Figure S2). Collectively, these studies confirmed that all Table 2 compounds effectively inhibited both COX and 5-LOX biosynthetic pathways with multiple compounds exhibiting balanced multitargeted activity in the low μM range. Finally, consistent with the relatively small size of these molecules, these compounds appeared to be generally brain-penetrant.

DISCUSSION

Although selected cholinesterase inhibitors and a single NMDA receptor antagonist are approved for the treatment of AD, these provide only a modest and temporary symptomatic improvement in AD patients and thus far there have been no examples of disease-modifying drug candidates for AD with demonstrated efficacy in phase III clinical trials.⁴³ This situation may be due, at least in part, to the fact that several neuropathological mechanisms are likely to provide potentially alternative or redundant pathways to drive/sustain the neurodegenerative process in AD. NSAIDs, for example, once attracted considerable attention as potential candidates for AD treatment due to promising results in a series of preclinical studies in animal models with Aβ plaque pathology,^{44–48} coupled with compelling retrospective epidemiological data indicating that individuals who were on sustained regimens of COX-inhibiting NSAIDs had reduced AD risk.^{45,49} A series of clinical trials with different COX inhibitors, however, yielded mostly disappointing results.^{45,50–52} Although there may be multiple reasons for the lack of efficacy in these clinical trials, including issues with the particular candidate compounds used in the studies and/or trials that were conducted in patient populations with disease that was too advanced to respond to this therapeutic approach, or who had dementia that was not due to underlying AD pathology, another possible mechanistic explanation may

be that even if substantial COX inhibition is achieved within the AD brain, this may not prevent the detrimental effects of inflammatory LTs. Indeed, different studies have now shown that these 5-LOX products are likely to contribute to Aβ plaque pathology,^{8,18,20,21,23} and there is evidence that blocking COX metabolism can lead to shunting of arachidonic acid to the 5-LOX pathway.^{53–55} Furthermore, it may be also argued that any potential benefit of lowering Aβ production and plaque pathology alone may be limited if tau pathology persists. Indeed, a recent retrospective analysis of several late-stage AD clinical trials, including the NSAIDs studies, concluded that candidate therapeutics affecting one target alone may not be likely to impact significantly disease progression,⁴³ suggesting that the evaluation and development of multitargeted approaches for AD would be desirable.⁵⁶ However, although different examples of multitargeted constructs have been proposed as experimental AD treatments, there have been only a few reports⁵⁷ of molecules that exhibit polypharmacology against targets that are likely involved in tau and Aβ neuropathology.

Prior studies suggested that axonal transport deficits associated with a loss of MTs and/or altered MT dynamics in the axon of neurons comprise a key neuropathological step of tauopathies and possibly other neurodegenerative diseases.²⁴ As part of our ongoing efforts to develop brain-penetrant MT-stabilizing agents as potential treatments for these diseases, we identified selected heterocyclic compounds that are not derived from natural products, as exemplified here by triazolopyrimidine 107⁵⁸ (Table 1), which exhibit a promising combination of MT-stabilizing activity and brain penetration.^{37,39} Among compound classes that are structurally and functionally related to the triazolopyrimidines are a series of 1,5-diarylimidazoles.³⁵ Like the triazolopyrimidines, these imidazoles are found to promote MT polymerization in cell-free assays and exhibit relatively potent and broad-spectrum fungicidal activity.³⁵ Furthermore, considering that these tricyclic compounds exhibit structural similarities with known NSAIDs, they may be considered as possible starting points in the development of small molecules that could concurrently stabilize MTs and lower eicosanoid production. Given that MT dynamics are believed to be affected in AD and other neurodegenerative disorders,^{24,59} and considering the involvement of

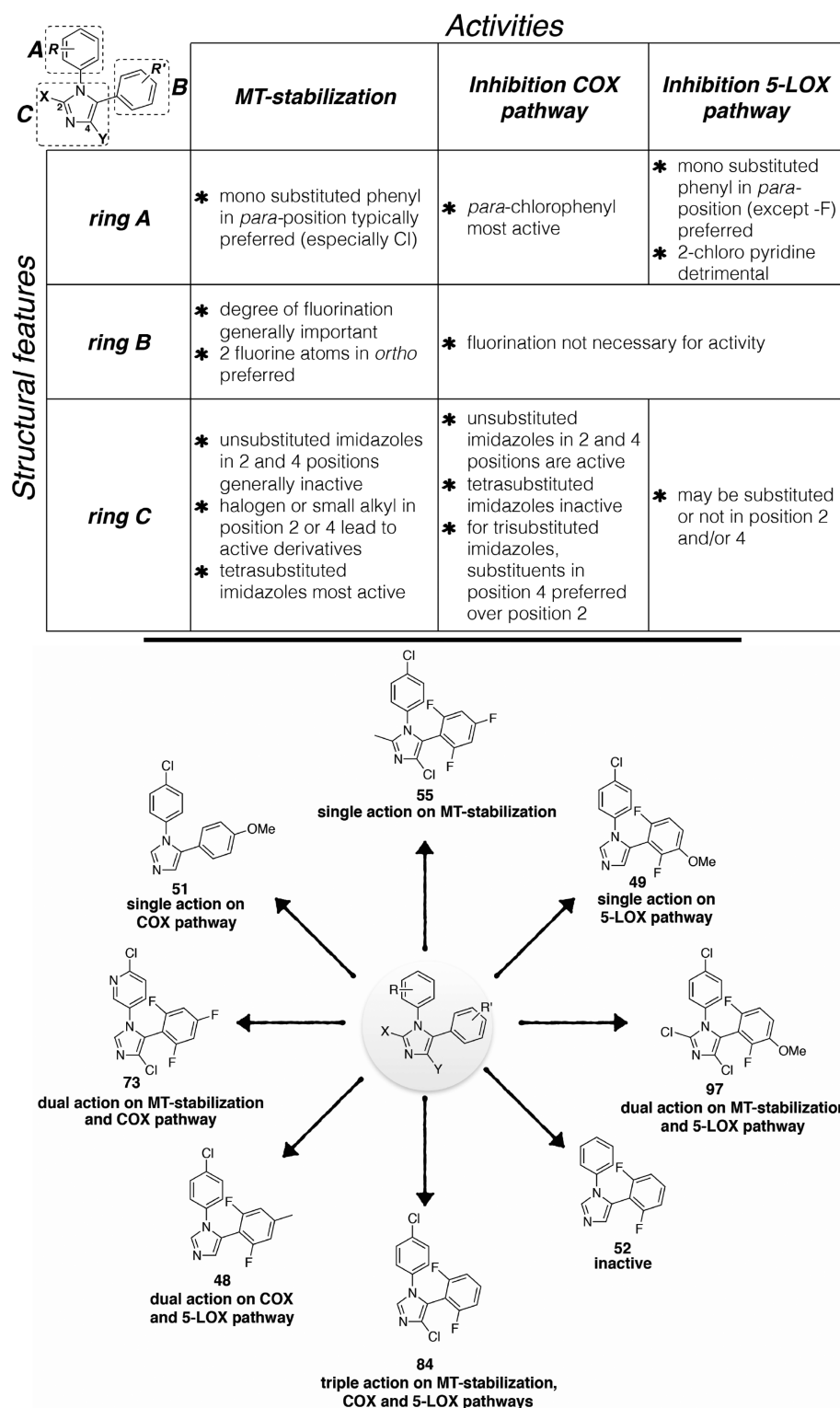


Figure 2. Summary of SARs (top) and representative structures exemplifying the different activity profiles exhibited by the 1,5-diarylimidazoles (bottom).

both COX- and 5-LOX derived eicosanoids in AD and likely other neurodegenerative diseases, a normalization of axonal MT dynamics, combined with a suppression of eicosanoid production, may provide a potential multitargeted strategy to mitigate concurrent disease mechanisms in AD and other neurodegenerative conditions.

Our multitargeted structure–activity relationship (SAR) studies began with the observation that selected examples from the

previously reported fungicidal imidazoles,³⁵ such as **2**, exhibit evidence of activity both as MT-stabilizing agents and inhibitors of eicosanoid biosynthesis *in vitro*, suggesting a potentially significant overlap between the pharmacophore of these MT-stabilizing imidazoles and that of NSAIDs such as **3** (COX-1 inhibitor³³). On the basis of these initial findings, and taking into consideration prior SAR studies³⁵ that defined a set of preferred substitutions on the imidazole ring that are

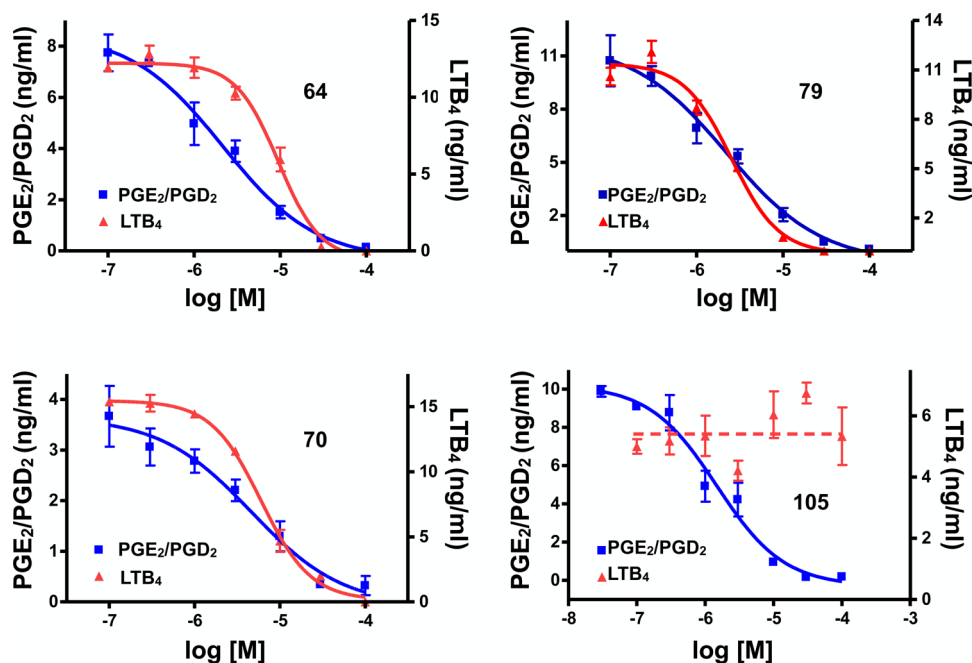


Figure 3. Representative dose–response curves in the RBL-1 cell assays. Samples were run in triplicate at each concentration, with the error bars representing standard error of the mean.

generally important for fungicidal activity, and thus presumably for MT-stabilizing activity, we focused on evaluating whether changes in the substitution patterns of 1,5-diarylimidazoles may result in compounds with improved and balanced multitargeted activities. In particular, given that optimal broad-spectrum fungicidal activity is typically achieved with tetrasubstituted imidazoles (e.g., **2**) and other related congeners that comprise a 4-chlorophenyl group at N1, a chlorine atom in position 4, and a di- or trifluorinated phenyl group in position 5, we focused primarily on evaluating (a) mono- and disubstitutions in the A ring, (b) chloro- and/or alkyl-substitutions in positions 2 and/or 4 of the imidazole ring, and (c) the effect of varying the degree and pattern of fluorination in the B ring. As shown in [Table 1](#), these studies demonstrated that relatively small changes in the substitution pattern of 1,5-diarylimidazoles can have profound effect in the activity profile of these molecules and ultimately led to the identification of several compounds with MT-stabilizing activity and inhibitory activity against the COX and/or 5-LOX pathways (see [Table 2](#)). Furthermore, with respect to the MT-stabilizing activity, our studies suggest that like the triazolopyrimidines, MT-stabilizing 1,5-diarylimidazoles are likely to affect MT structures in different ways depending on the particular substitution pattern. In the case of triazolopyrimidines, it was suggested that congeners bearing an alkoxy side chain in the fluorinated phenyl ring (e.g., **108**) typically produce an unusual cellular phenotype that is characterized by a bell-shaped concentration–response relationship in the AcTub assay and proteasome-dependent degradation of α - and β -tubulin.³⁹ Interestingly, a similar type of observation is seen with the 1,5-diarylimidazoles, as all MT-active compounds bearing an alkoxy substituent in ring B (i.e., **2**, **58**, **95–97**, [Table 1](#)) produce a loss in α -tubulin at compound concentrations that are required to observe an increase in AcTub. However, our results with the 1,5-diarylimidazoles clearly suggest that the substitution pattern of ring B may not be the only determining factor in whether α -tubulin is affected, as other substitutions in the A and C ring appear to play a role

(e.g., compare **29** with **30**, and **54** with **73**, [Table 1](#)). As was noted for the triazolopyrimidines,³⁹ compounds found to cause a reduction in total tubulin may not be desirable for neurodegenerative diseases as this effect would be expected to ultimately compromise rather than restore axonal MT function. Conversely, certain multitargeted congeners, including examples listed in [Table 2](#) that do not appear to reduce total α -tubulin levels at concentrations that increase AcTub, may be more promising candidates for tauopathy treatment. Further studies, however, will be necessary to confirm that these compounds can produce beneficial effects in an animal model of tau pathology, as observed previously with MT-stabilizing natural products like paclitaxel,⁶⁰ epothilone D, and dictyostatin.^{4–7}

With respect to the ability of these compounds to act as inhibitors of the COX and/or 5-LOX pathways, although the IC_{50} values in the COX biosynthetic pathway assay are much higher than the IC_{50} of COX inhibitor **3** (i.e., ~ 1 nM), the activity level displayed by these molecules is closely comparable to that of the over-the-counter drug, ibuprofen (**105**; [Table 1](#) and [Figure 3](#)). Unlike **105** or **3**, however, these multitargeted 1,5-diarylimidazoles (e.g., **79**, see [Table 2](#) and [Figure 3](#)) exhibit inhibition activity against the leukotriene biosynthetic pathway, while other derivatives ([Table 2](#)) are also capable of affecting MT stability in vitro, with several examples (e.g., **68**, **70**, **87**) exhibiting relatively balanced multitargeted activity. Moreover, an evaluation of the brain penetration of these molecules revealed that these multitargeted prototypes are generally capable of reaching significant brain concentrations after peripheral administration, suggesting that compounds of this type may be appropriate for further evaluation in the context of CNS diseases. Taken together, these results indicate that these 1,5-diarylimidazoles comprise a promising scaffold for the evaluation of CNS-directed multitargeted strategies that either focus on a concurrent inhibition of COX and 5-LOX biosynthetic pathways or on a combined stabilization of MTs and inhibition of eicosanoid production.

Table 2. Further Evaluation of Test Compounds with Multitargeted Activity as MT-Stabilizing Agents and/or Inhibitors of COX and 5-LOX Pathways

	Cpd#	Structure	PGD ₂ /E ₂ Inhibition IC ₅₀ (μM) ^a	LTB ₄ Inhibition IC ₅₀ (μM) ^a	Relative Change in AcTub ^b	Brain (nM)	Plasma (nM)	B/P
Multi-targeted Compounds with Activity as MT-Stabilizing Agents and Inhibitors of COX and 5-LOX Pathways	29		12.1	13.4	× 3.5 (10 μM)	600 [^] ± 200	500 [^] ± 300	1.4 ± 0.3
	35		4.7	23.7	× 3.4 (10 μM)	400 [^] ± 200	200 [^] ± 100	1.9 ± 0.2
	59		2.4	9.7	× 4.1 (10 μM)	ND	ND	ND
	60		9.8	20.8	× 3.4 (10 μM)	210 [^] ± 90	210 [^] ± 80	0.9 ± 0.1
	64		2.2	9.5	× 2.4 (10 μM)	400 [#] ± 200	190 [#] ± 90	2.1 ± 0.5
	67		6.5	7.8	× 2.1 (10 μM)	240 [#] ± 100	260 [#] ± 90	0.9 [#] ± 0.2
	68		2.9	2.4	× 2.0 (10 μM)	700 [#] ± 500	300 [#] ± 200	2.8 ± 0.8
	70		4.6	6.0	× 1.9 (10 μM)	700 [#] ± 200	240 [#] ± 50	3.0 ± 1.0
	84		2.4	13.8	× 4.0 (10 μM)	700 [^] ± 400	400 [^] ± 200	1.9 ± 0.2
	87		15.0	10.7	× 4.8 (10 μM)	900 [#] ± 300	480 [#] ± 60	1.9 ± 0.4
92		1.8	11.7	× 3.6 (10 μM)	300 [^] ± 100	110 [^] ± 60	2.5 ± 0.1	
Dual Inhibitors of COX/5-LOX Pathways	79		2.2	2.5	NS	200 [^] ± 80	60 [^] ± 30	3.3 ± 0.1
	98		1.0	12.5	NS	200 [^] ± 60	80 [^] ± 20	2.4 ± 0.1

Table 2. continued

^aAll concentration–response analyses were conducted at multiple concentrations with triplicate samples per concentration. ^bThe change in AcTub was assessed as described in Table 1. [†] Study conducted after a 5 mg/kg i.p. injection of test compound. [^] Study conducted after a 2 mg/kg i.p. injection of test compound with drug concentrations adjusted proportionally upward to allow comparison to 5 mg/kg doses. ND, not determined. NS, not significant. \pm errors represent standard deviations. All analyses were conducted with groups of three mice.

CONCLUSIONS

Starting from a series of 1,5-diarylimidazoles with reported MT-stabilizing activity and structural similarities with known NSAIDs, the SAR studies reported here led to the identification of a series of congeners that exhibit balanced low μ M in vitro activity as MT-stabilizing agents and/or inhibitors of the COX and 5-LOX pathways. Given that prior preclinical studies demonstrated that MT stabilization in neurons is a promising therapeutic strategy to treat tau-mediated neurodegeneration, combined with the considerable body of evidence implicating eicosanoids in A β plaque pathology, the balanced polypharmacology and brain penetration displayed by these compounds suggest that they are promising research tools as well as possible lead structures to investigate multitargeted therapeutic approaches for AD.

EXPERIMENTAL SECTION

Materials and Methods. All solvents were reagent grade. All reagents were purchased from Aldrich or Acros and used as received. Thin layer chromatography (TLC) was performed with 0.25 mm E. Merck precoated silica gel plates. Silica gel column chromatography was performed with silica gel 60 (particle size 0.040–0.062 mm) supplied by Silicycle and Sorbent Technologies. TLC spots were detected by viewing under a UV light. Melting points (mp) were acquired on a Thomas–Hoover apparatus and are uncorrected. Infrared (IR) spectra were recorded on a Jasco model FT/IR-480 Plus spectrometer. Proton (¹H) and carbon (¹³C) NMR spectra were recorded on a Bruker AMX-500 spectrometer. Chemical shifts were reported relative to solvents. High-resolution mass spectra were measured at the University of Pennsylvania Mass Spectrometry Center on either a VG Micromass 70/70H or VG ZAB-E spectrometer. Single-crystal X-ray structure determinations were performed at the University of Pennsylvania with an Enraf Nonius CAD-4 diffractometer. Analytical reverse-phase (Sunfire C18; 4.6 mm \times 50 mm, 5 mL) high-performance liquid chromatography (HPLC) was performed with a Waters binary gradient module 2525 equipped with Waters 2996 PDA and Waters micromass ZQ. All samples were analyzed employing a linear gradient from 10% to 90% of CH₃CN in water over 8 min and flow rate of 1 mL/min, and unless otherwise stated, the purity level was >95%. Preparative reverse-phase HPLC purifications were performed on a Gilson instrument (i.e., Gilson 333 pumps, a 215 liquid handler, 845Z injection module, and PDA detector) employing Waters SunFire preparative C₁₈ OBD columns (5 μ m 19 mm \times 50 mm or 19 mm \times 100 mm). Purifications were carried out employing a linear gradient from 10% to 90% of CH₃CN in water for 15 min with a flow rate of 20 mL/min. Unless otherwise stated, all final compounds were found to be >95% pure as determined by HPLC/MS and NMR.

General Procedure A for the Synthesis of Imines. A solution of aniline (1 equiv) and benzaldehyde (1 equiv) in toluene (0.2 M) was heated at 110 °C in a Dean–Stark apparatus for 4 days. The reaction mixture was then cooled and evaporated in vacuo to obtain the title compound, which was used in the next step without further purification.

General Procedure B for the Synthesis of Imines. To a solution of a primary amine (1 equiv) in anhydrous Et₂O (0.3 M) in the presence of molecular sieves (4 Å, 1.6 mm pellets, 7 g/mmol) was added an aldehyde (1 equiv) according to the Taguchi's method. The mixture was heated and stirred at 30 °C for 48 h. Molecular sieves were then removed by filtration, and the solvent was evaporated in vacuo to afford the desired imine in quantitative yields.

General Procedure C for the Synthesis of Imidazoles. To a solution of imine (1 equiv) in a mixture of DMF (0.26 M) and 1,2-dimethoxyethane (0.32 M) were added toluenesulfonylmethyl isocyanide (1.5 equiv) and anhydrous K₂CO₃ (2.08 equiv). The reaction mixture was heated for 16 h at 100 °C, then cooled to rt, filtered, and evaporated in vacuo. The resulting material was adsorbed on Celite 545 AW and purified by silica gel column chromatography to obtain the desired compound.

General Procedure D for the Synthesis of 4-Alkylated Imidazoles. To a solution of imine (1 equiv) in a mixture of DMF (0.14 M) and 1,2-dimethoxyethane (0.17 M) were added 1-((1-isocyanoethyl)sulfonyl)-4-methylbenzene (1.5 equiv) and anhydrous K₂CO₃ (2.08 equiv). The reaction mixture was heated for 16 h at 100 °C, then cooled to rt, filtered through a pad of Celite 545 AW, and evaporated in vacuo. The resulting material was purified by silica gel column chromatography to obtain the desired compound.

General Procedure E for the Mono- and Dichlorination of 1,5-Diarylimidazoles. To a solution of imidazole (1 equiv) in CHCl₃ (0.16 M) was added N-chlorosuccinimide (1.06 equiv). The reaction mixture was heated at 60 °C for 16 h, then cooled to rt and diluted with EtOAc. The organic layer was washed with brine (\times 3), dried over MgSO₄, filtered, and evaporated in vacuo. Purification via silica gel column chromatography furnished the mono- and dichlorinated imidazoles.

General Procedure F for Alkylation of 1,5-Diarylimidazoles. To a solution of diisopropylamine (1.5 equiv) in THF (0.3 M) at –20 °C was added *n*-BuLi (2.5 M in hexanes, 1.5 equiv), and the mixture was stirred for 10 min. A solution of imidazole (1 equiv) in THF (0.15 M) was added, and after stirring for 30 min, methyl iodide or ethyl iodide (3 equiv) was added. The mixture was stirred for 30 min at –20 °C and for 30 min at rt. H₂O was then added to the reaction mixture. The aqueous phase was extracted with EtOAc, and the combined organic layers were washed with brine (\times 3), dried over MgSO₄, filtered, and concentrated in vacuo. Purification via silica gel column chromatography furnished the desired alkylated imidazoles.

4-Chloro-1-(4-chlorophenyl)-5-(2,6-difluoro-4-methoxyphenyl)-2-methyl-1H-imidazole (2). To a solution of 4-chloro-1-(4-chlorophenyl)-2-methyl-5-(2,4,6-trifluorophenyl)-1H-imidazole (0.004 g, 0.011 mmol) in THF (0.011 mL) at 0 °C was added a 30% sodium methoxide solution in MeOH (0.007 mL). The reaction mixture was stirred for 19 h at rt, then quenched with an aqueous ammonium chloride solution and extracted with EtOAc (\times 3). The combined organic layers were dried (MgSO₄), filtered, and concentrated in vacuo. The crude products were purified by preparative reverse-phase HPLC to obtain the title compound as a white solid (0.004 g, 0.011 mmol, 97% yield). ¹H NMR (500 MHz, CDCl₃) δ 7.40 (d, *J* = 8.5 Hz, 2H), 7.11 (d, *J* = 8.5 Hz, 2H), 6.41 (d, *J* = 9.1 Hz, 2H), 3.78 (s, 3H), 2.41 (s, 3H) ppm. ¹³C NMR (126 MHz, CDCl₃) δ 163.04 (t, *J* = 14.0 Hz), 161.61 (dd, *J* = 249.5, 8.9 Hz), 145.57, 136.11, 133.46, 130.11, 129.90, 128.65, 128.38, 127.63, 117.32, 98.38 (d, *J* = 28.0 Hz), 96.57 (t, *J* = 20.8 Hz), 56.09, 13.37 ppm. IR (KBr) ν 2962, 2928, 2852, 1646, 1575, 1494, 1448, 1152 cm^{–1}. HRMS (ES⁺) calculated for C₁₇H₁₃Cl₂F₂N₂O [M + H]⁺ 369.0373, found 369.0374.

(E)-N-(4-Chlorophenyl)-1-(2,4,6-trifluorophenyl)methanimine (5). Following synthetic procedure A using 4-chloroaniline (0.829 g, 6.50 mmol) and 2,4,6-trifluorobenzaldehyde (1.04 g, 6.50 mmol), the title compound was obtained as a brown solid (1.75 g, 6.49 mmol, 99% yield). ¹H NMR (500 MHz, CDCl₃) δ 8.51 (s, 1H), 7.32 (app d, *J* = 6.7 Hz, 2H), 7.12 (app d, *J* = 6.8 Hz, 2H), 6.73 (m, 2H) ppm.

(E)-N-(4-Methoxyphenyl)-1-(2,4,6-trifluorophenyl)methanimine (6). Following synthetic procedure A using 4-methoxyaniline (0.370 g, 3.00 mmol) and 2,4,6-trifluorobenzaldehyde (0.480 g, 3.00 mmol), the title compound was obtained as a brown solid (0.814 g, 3.07 mmol,

99% yield). ^1H NMR (500 MHz, CDCl_3) δ 8.59 (s, 1H), 7.25–7.22 (m, 2H), 6.97–6.90 (m, 2H), 6.81–6.72 (m, 2H), 3.84 (s, 3H) ppm.

(E)-N-(4-Chlorophenyl)-1-(2,6-difluoro-3-methylphenyl)methanimine (7). Following synthetic procedure A using 4-chloroaniline (0.383 g, 3 mmol) and 2,6-difluoro-3-methylbenzaldehyde (0.377 mL, 3 mmol), the title compound was obtained as a brown solid (0.781 g, 2.94 mmol, 98% yield). ^1H NMR (500 MHz, CDCl_3) δ 8.63 (s, 1H), 7.36 (app d, $J = 8.2$ Hz, 2H), 7.25 (app q, $J = 7.6$ Hz, 1H), 7.17 (app d, $J = 8.0$ Hz, 2H), 6.89 (app t, $J = 9.2$ Hz, 1H), 2.28 (s, 3H) ppm.

(E)-1-(3-Chloro-2,6-difluorophenyl)-N-(4-chlorophenyl)methanimine (8). Following synthetic procedure A using 4-chloroaniline (0.383 g, 3 mmol) and 3-chloro-2,6-difluorobenzaldehyde (0.530 g, 3 mmol), the title compound was obtained as a brown solid (0.850 g, 2.97 mmol, 99% yield). ^1H NMR (500 MHz, CDCl_3) δ 8.60 (s, 1H), 7.47 (td, $J = 8.4, 5.5$ Hz, 1H), 7.37 (app d, $J = 8.5$ Hz, 2H), 7.17 (app d, $J = 8.5$ Hz, 2H), 7.00–6.96 (m, 1H) ppm. ^{13}C NMR (126 MHz, CDCl_3) δ 159.87 (dd, $J = 390.8, 5.6$ Hz), 157.80 (dd, $J = 393.2, 5.6$ Hz), 150.87, 150.42, 132.72 (d, $J = 10.3$ Hz), 132.65, 129.47, 122.29, 117.77 (dd, $J = 18.0, 3.9$ Hz), 115.03 (t, $J = 12.9$ Hz), 112.80 (dd, $J = 23.0, 4.4$ Hz) ppm.

(E)-1-(3-Bromo-2,6-difluorophenyl)-N-(4-chlorophenyl)methanimine (9). Following synthetic procedure A using 4-chloroaniline (0.383 g, 3 mmol) and 3-bromo-2,6-difluorobenzaldehyde (0.663 g, 3 mmol), the title compound was obtained as a brown solid (0.971 g, 2.94 mmol, 98% yield). ^1H NMR (500 MHz, CDCl_3) δ 8.59 (s, 1H), 7.61 (dd, $J = 14.2, 7.6$ Hz, 1H), 7.36 (app d, $J = 8.5$ Hz, 2H), 7.17 (app d, $J = 8.4$ Hz, 2H), 6.93 (t, $J = 9.2$ Hz, 1H) ppm.

(E)-N-(4-Chlorophenyl)-1-(2,3,6-trifluorophenyl)methanimine (10). Following synthetic procedure A using 4-chloroaniline (0.383 g, 3 mmol) and 2,3,6-trifluorobenzaldehyde (0.337 mL, 3 mmol), the title compound was obtained as a brown solid (0.778 g, 2.88 mmol, 96% yield). ^1H NMR (500 MHz, CDCl_3) δ 8.58 (s, 1H), 7.34 (app d, $J = 8.3$ Hz, 2H), 7.26–7.20 (m, 1H), 7.16 (app d, $J = 8.2$ Hz, 2H), 6.92 (app t, $J = 9.0$ Hz, 1H) ppm. ^{13}C NMR (126 MHz, CDCl_3) δ 158.28, 156.26, 150.76, 150.19, 148.36–148.23 (m), 146.34 (dd, $J = 12.5, 3.6$ Hz), 132.51, 129.30, 122.18, 119.33 (dd, $J = 19.4, 10.4$ Hz), 115.07 (dd, $J = 14.2, 9.0$ Hz), 111.42 (dt, $J = 24.4, 5.3$ Hz) ppm.

(E)-N-(4-Chloro-3-fluorophenyl)-1-(2,3,6-trifluorophenyl)methanimine (11). Following synthetic procedure A using 4-chloro-3-fluoroaniline (0.437 g, 3 mmol) and 2,3,6-trifluorobenzaldehyde (0.337 mL, 3 mmol), the title compound was obtained as a brown solid (0.846 g, 2.94 mmol, 98% yield).

(E)-N-(6-Chloropyridin-3-yl)-1-(2,4,6-trifluorophenyl)methanimine (12). Following synthetic procedure A using 6-chloropyridin-3-amine (0.385 g, 3 mmol) and 2,4,6-trifluorobenzaldehyde (0.480 g, 3 mmol), the title compound was obtained as a brown solid (0.786 g, 2.90 mmol, 97% yield).

(E)-N-(4-Chlorophenyl)-1-(4-fluorophenyl)methanimine (13). Following synthetic procedure A using 4-chloroaniline (0.383 g, 3 mmol) and 4-fluorobenzaldehyde (0.322 mL, 3 mmol), the title compound was obtained as a brown solid (0.687 g, 2.94 mmol, 98% yield).

(E)-N-(4-Chloro-2-fluorophenyl)-1-(2,6-difluorophenyl)methanimine (14). Following synthetic procedure A using 4-chloro-2-fluoroaniline (0.437 g, 3 mmol) and 2,6-difluorobenzaldehyde (0.426 g, 3 mmol), the title compound was obtained as a brown solid (0.768 g, 2.85 mmol, 95% yield).

(E)-N-(4-Chlorophenyl)-1-(2,5-difluorophenyl)methanimine (15). Following synthetic procedure A using 4-chloroaniline (0.383 g, 3 mmol) and 2,5-difluorobenzaldehyde (0.326 mL, 3 mmol), the title compound was obtained as a brown solid (0.698 g, 2.77 mmol, 93% yield). ^1H NMR (500 MHz, CDCl_3) δ 8.66 (s, 1H), 7.84 (dt, $J = 7.6, 4.2$ Hz, 1H), 7.35 (d, $J = 8.4$ Hz, 2H), 7.17 (d, $J = 8.4$ Hz, 2H), 7.14–7.06 (m, 2H) ppm. ^{13}C NMR (126 MHz, CDCl_3) δ 159.88, 157.92 (dd, $J = 7.7, 1.9$ Hz), 152.39 (d, $J = 1.2$ Hz), 149.67, 132.37, 131.65 (d, $J = 16.8$ Hz), 129.36, 129.11 (dd, $J = 51.2, 13.4$ Hz), 125.04 (dd, $J = 11.3, 7.8$ Hz), 122.40 (d, $J = 19.7$ Hz), 119.85 (dd, $J = 24.9, 9.0$ Hz), 117.27 (dd, $J = 24.0, 8.3$ Hz), 113.64 (dd, $J = 25.1, 2.9$ Hz) ppm.

(E)-1-(2,6-Difluorophenyl)-N-(4-(trifluoromethoxy)phenyl)methanimine (16). Following synthetic procedure A using 4-(trifluoromethoxy)aniline (0.531 g, 3.00 mmol) and 2,6-difluoro-

benzaldehyde (0.426 g, 3.00 mmol), the title compound was obtained as a brown liquid (1.034 g, 3.43 mmol, 99% yield). ^1H NMR (500 MHz, CDCl_3) δ 8.65 (s, 1H), 7.46–7.39 (m, 1H), 7.26–7.22 (m, 4H), 7.01 (t, $J = 8.6$ Hz, 2H) ppm.

(E)-N-(4-Chlorophenyl)-1-(2,6-difluorophenyl)methanimine (17). Following synthetic procedure A using 4-chloroaniline (0.829 g, 6.50 mmol) and 2,6-difluorobenzaldehyde (0.924 g, 6.50 mmol), the title compound was obtained as a brown liquid (1.62 g, 6.45 mmol, 99% yield). ^1H NMR (500 MHz, CDCl_3) δ 8.64 (s, 1H), 7.46–7.40 (m, 1H), 7.40–7.34 (m, 2H), 7.20–7.14 (m, 2H), 7.04–6.96 (m, 2H) ppm.

(E)-N-(4-(Trifluoromethoxy)phenyl)-1-(2,3,6-trifluorophenyl)methanimine (18). Following synthetic procedure A using 4-(trifluoromethoxy)aniline (0.531 g, 3.00 mmol) and 2,3,6-trifluorobenzaldehyde (0.480 g, 3.00 mmol), the title compound was obtained as a brown solid (1.08 g, 3.47 mmol, 99% yield). ^1H NMR (500 MHz, CDCl_3) δ 8.62 (s, 1H), 7.45–7.25 (m, 2H), 7.27–7.22 (m, 2H), 7.20–7.11 (m, 1H), 7.02–6.93 (m, 1H) ppm.

(E)-N-(4-Chlorophenyl)-1-(2,6-difluoro-4-methylphenyl)methanimine (19). Following synthetic procedure A using 4-chloroaniline (0.157 g, 1.23 mmol) and 2,6-difluoro-4-methylbenzaldehyde (0.192 g, 3 mmol), the title compound was obtained as a brown solid (0.183 g, 0.69 mmol, 56% yield). ^1H NMR (500 MHz, CDCl_3) δ 8.59 (s, 1H), 7.36 (d, $J = 8.2$ Hz, 2H), 7.15 (d, $J = 8.2$ Hz, 2H), 6.82 (d, $J = 10.1$ Hz, 2H), 2.40 (s, 3H) ppm.

(E)-N-(4-Chlorophenyl)-1-(2,6-difluoro-3-methoxyphenyl)methanimine (20). Following synthetic procedure A using 4-chloroaniline (0.383 g, 3.00 mmol) and 2,6-difluoro-3-methoxybenzaldehyde (0.468 g, 3.00 mmol), the title compound was obtained as a brown solid (0.745 g, 2.64 mmol, 88% yield). ^1H NMR (500 MHz, CDCl_3) δ 8.63 (s, 1H), 7.39–7.32 (m, 2H), 7.20–7.11 (m, 2H), 7.07–6.98 (m, 1H), 6.96–6.87 (m, 1H), 3.90 (s, 3H) ppm.

(E)-N-(4-Chlorophenyl)-1-phenylmethanimine (21). Following synthetic procedure A using 4-chloroaniline (0.383 g, 3.00 mmol) and benzaldehyde (0.318 g, 3.00 mmol), the title compound was obtained as a brown solid (0.702 g, 3.25 mmol, 99% yield). ^1H NMR (500 MHz, CDCl_3) δ 8.44 (s, 1H), 7.96–7.87 (m, 2H), 7.57–7.45 (m, 3H), 7.36 (d, $J = 8.3$ Hz, 2H), 7.16 (d, $J = 8.3$ Hz, 2H) ppm.

(E)-N-(4-Chlorophenyl)-1-(4-methoxyphenyl)methanimine (22). Following synthetic procedure B using 4-chloroaniline (0.765 g, 6.00 mmol) and 4-methoxybenzaldehyde (0.817 g, 6.00 mmol), the title compound was obtained as a yellow solid (1.370 g, 5.58 mmol, 93% yield). ^1H NMR (500 MHz, CDCl_3) δ 8.35 (s, 1H), 7.84 (d, $J = 8.4$ Hz, 2H), 7.37–7.31 (m, 2H), 7.13 (d, $J = 8.5$ Hz, 2H), 6.98 (d, $J = 8.4$ Hz, 2H), 3.87 (s, 3H) ppm.

(E)-1-(2,6-Difluorophenyl)-N-phenylmethanimine (23). Following synthetic procedure B using aniline (0.559 g, 6.00 mmol) and 2,6-difluorobenzaldehyde (0.853 g, 6.00 mmol), the title compound was obtained as a yellow liquid (0.637 g, 2.93 mmol, 49% yield). ^1H NMR (500 MHz, CDCl_3) δ 8.65 (s, 1H), 7.44–7.34 (m, 3H), 7.26–7.19 (m, 3H), 7.02–6.95 (m, 2H) ppm.

(E)-N-(2-Chlorophenyl)-1-(2,6-difluorophenyl)methanimine (24). Following synthetic procedure B using 2-chloroaniline (0.765 g, 6.00 mmol) and 2,6-difluorobenzaldehyde (0.853 g, 6.00 mmol), the title compound was obtained as a yellow liquid (1.41 g, 5.58 mmol, 93% yield). ^1H NMR (500 MHz, CDCl_3) δ 8.62 (s, 1H), 7.49–7.39 (m, 2H), 7.32–7.27 (m, 1H), 7.20–7.14 (m, 1H), 7.06–6.98 (m, 3H) ppm.

1-(4-Chlorophenyl)-5-(2,4,6-trifluorophenyl)-1H-imidazole (25). Following synthetic procedure C using (E)-N-(4-chlorophenyl)-1-(2,4,6-trifluorophenyl)methanimine (0.865 g, 3.21 mmol), purification by silica gel column chromatography (hexanes/EtOAc 100:0 to 60:40) afforded the title compound as a white powder (0.429 g, 1.39 mmol, 43% yield). ^1H NMR (500 MHz, CDCl_3) δ 7.98 (s, 1H), 7.39–7.36 (m, 2H), 7.35 (s, 1H), 7.13–7.10 (m, 2H), 6.71–6.65 (m, 2H) ppm. ^{13}C NMR (126 MHz, CDCl_3) δ 163.14 (dt, $J = 252.4, 15.3$ Hz), 160.75 (ddd, $J = 251.5, 14.9, 8.7$ Hz), 138.95, 134.96, 134.41, 132.41, 129.76, 125.94, 119.16, 103.78 (td, $J = 20.0, 4.6$ Hz), 100.97–100.52 (m) ppm. IR (KBr) ν 3114, 3095, 3043, 2922, 1692, 1644, 1600, 1562,

2,4-Dichloro-1-(4-chlorophenyl)-5-(2,4,6-trifluorophenyl)-1H-imidazole (57). Following synthetic procedure E using 1-(4-chlorophenyl)-5-(2,4,6-trifluorophenyl)-1H-imidazole (0.400 g, 1.3 mmol), purification by silica gel column chromatography (hexanes/EtOAc 100:0 to 70:30) afforded the title compound as a white solid (0.016 g, 0.042 mmol, 3% yield). ^1H NMR (500 MHz, CDCl_3) δ 7.39–7.36 (m, 2H), 7.12 (d, J = 8.6 Hz, 2H), 6.69–6.63 (m, 2H) ppm. ^{13}C NMR (126 MHz, CDCl_3) δ 164.23 (dt, J = 254.2, 15.3 Hz), 161.26 (ddd, J = 253.1, 15.1, 8.3 Hz), 136.22, 132.94, 132.88, 130.83, 129.91, 128.57, 117.68, 101.61 (td, J = 20.2, 4.9 Hz), 101.23–100.78 (m) ppm. IR (KBr) ν 3100, 3067, 2962, 2928, 2857, 1645, 1599, 1495, 1446, 1121, 1038, 998 cm^{-1} . HRMS (ES^+) calculated for $\text{C}_{15}\text{H}_7\text{Cl}_3\text{F}_3\text{N}_2$ [$\text{M} + \text{H}$] $^+$ 376.9627, found 376.9627.

2,4-Dichloro-1-(4-chlorophenyl)-5-(2,6-difluoro-4-methoxyphenyl)-1H-imidazole (58). To a solution of 2,4-dichloro-1-(4-chlorophenyl)-5-(2,4,6-trifluorophenyl)-1H-imidazole (0.032 g, 0.085 mmol) in THF (0.53 mL) at 0 °C was added a 30% sodium methoxide solution in MeOH (0.031 mL). The reaction mixture was stirred for 16 h at rt, then quenched with an aqueous ammonium chloride solution and extracted with EtOAc (3 \times). The combined organic layers were dried (Na_2SO_4), filtered, and concentrated. The crude products were purified by preparative reverse-phase HPLC to obtain the title compound as a white solid (0.011 g, 0.028 mmol, 33% yield). ^1H NMR (500 MHz, CDCl_3) δ 7.38–7.35 (m, 2H), 7.12 (d, J = 8.6 Hz, 2H), 6.41 (q, J = 7.3 Hz, 2H), 3.78 (s, 3H) ppm. ^{13}C NMR (126 MHz, CDCl_3) δ 162.97 (t, J = 14.0 Hz), 161.59 (dd, J = 249.7, 9.1 Hz), 135.90, 133.24, 132.20, 130.42, 129.75, 118.83, 101.00 (td, J = 26.4, 3.1 Hz), 98.46–98.24 (m), 97.03 (t, J = 20.6 Hz), 56.07 ppm. IR (KBr) ν 3390, 2965, 2924, 2848, 1644, 1574, 1495, 1445, 1384, 1352, 1150 cm^{-1} . HRMS (ES^+) calculated for $\text{C}_{16}\text{H}_{10}\text{Cl}_3\text{F}_2\text{N}_2\text{O}$ [$\text{M} + \text{H}$] $^+$ 388.9827, found 388.9830.

4-Chloro-1-(4-methoxyphenyl)-5-(2,4,6-trifluorophenyl)-1H-imidazole (59). Following synthetic procedure E using 1-(4-methoxyphenyl)-5-(2,4,6-trifluorophenyl)-1H-imidazole (0.086 g, 0.283 mmol), purification by silica gel column chromatography (hexanes/EtOAc 80:20) afforded the title compound as a yellow solid (0.043 g, 0.127 mmol, 45% yield). ^1H NMR (500 MHz, CDCl_3) δ 7.64 (s, 1H), 7.06 (d, J = 8.6 Hz, 2H), 6.88–6.82 (m, 2H), 6.71–6.61 (m, 2H), 3.79 (s, 3H) ppm. ^{13}C NMR (126 MHz, CDCl_3) δ 163.80 (dt, J = 252.7, 15.1 Hz), 161.21 (ddd, J = 252.7, 15.3, 8.6 Hz), 159.90, 137.20, 131.91, 128.82, 126.27, 115.50, 114.71, 102.27 (td, J = 20.4, 4.7 Hz), 101.15–100.40 (m), 55.62 ppm. IR (KBr) ν 3149, 3047, 2983, 2941, 2916, 2838, 1644, 1595, 1564, 1517, 1468, 1439, 1249, 1179, 1128, 1028 cm^{-1} . HRMS (ES^+) calculated for $\text{C}_{16}\text{H}_{11}\text{ClF}_3\text{N}_2\text{O}$ [$\text{M} + \text{H}$] $^+$ 339.0512, found 339.0481.

2-Chloro-1-(4-methoxyphenyl)-5-(2,4,6-trifluorophenyl)-1H-imidazole (60). Following synthetic procedure E using 1-(4-methoxyphenyl)-5-(2,4,6-trifluorophenyl)-1H-imidazole (0.086 g, 0.283 mmol), purification by silica gel column chromatography (hexanes/EtOAc 80:20) afforded the title compound as a yellow solid (0.015 g, 0.044 mmol, 16% yield). ^1H NMR (500 MHz, CDCl_3) δ 7.14 (s, 1H), 7.11–7.06 (m, 2H), 6.89–6.84 (m, 2H), 6.64–6.56 (m, 2H), 3.81 (s, 3H) ppm. ^{13}C NMR (126 MHz, CDCl_3) δ 163.34 (dt, J = 252.7, 15.4 Hz), 161.13 (ddd, J = 251.5, 15.0, 8.5 Hz), 160.07, 134.94, 130.16, 128.51, 127.52, 121.78, 114.42, 103.86 (td, J = 20.3, 4.7 Hz), 101.08–100.00 (m), 55.59 ppm. IR (KBr) ν 3053, 2962, 2917, 2847, 1645, 1596, 1570, 1514, 1485, 1448, 1253, 1171, 1124, 1035 cm^{-1} . HRMS (ES^+) calculated for $\text{C}_{16}\text{H}_{11}\text{ClF}_3\text{N}_2\text{O}$ [$\text{M} + \text{H}$] $^+$ 339.0512, found 339.0499.

2,4-Dichloro-1-(4-methoxyphenyl)-5-(2,4,6-trifluorophenyl)-1H-imidazole (61). Following synthetic procedure E using 1-(4-methoxyphenyl)-5-(2,4,6-trifluorophenyl)-1H-imidazole (0.086 g, 0.283 mmol), purification by silica gel column chromatography (hexanes/EtOAc 80:20) afforded the title compound as a yellow solid (0.010 g, 0.027 mmol, 9% yield). ^1H NMR (500 MHz, CDCl_3) δ 7.11–7.06 (m, 2H), 6.89–6.84 (m, 2H), 6.67–6.60 (m, 2H), 3.81 (s, 3H) ppm. ^{13}C NMR (126 MHz, CDCl_3) δ 164.01 (dt, J = 253.2, 15.2 Hz), 161.30 (ddd, J = 252.8, 14.8, 8.5 Hz), 160.40, 133.20, 131.10, 130.15, 128.99, 128.46, 127.07, 117.87, 114.60, 101.95 (td, J = 20.2, 4.6 Hz), 101.36–100.34 (m), 55.63 ppm. IR (KBr) ν 2960, 2918,

2849, 1643, 1513, 1445, 1255, 1121, 1036 cm^{-1} . HRMS (ES^+) calculated for $\text{C}_{16}\text{H}_{10}\text{Cl}_2\text{F}_3\text{N}_2\text{O}$ [$\text{M} + \text{H}$] $^+$ 373.0122, found 373.0112.

4-Chloro-1-(4-chlorophenyl)-5-(2,6-difluoro-3-methylphenyl)-1H-imidazole (62). Following synthetic procedure E using 1-(4-chlorophenyl)-5-(2,6-difluoro-3-methylphenyl)-1H-imidazole (0.326 g, 1.07 mmol), purification by silica gel column chromatography (hexanes/EtOAc 100:0 to 80:20) afforded the title compound as a beige solid (0.187 g, 0.551 mmol, 52% yield). ^1H NMR (500 MHz, CDCl_3) δ 7.73 (s, 1H), 7.36–7.33 (m, 2H), 7.22 (q, J = 7.5 Hz, 1H), 7.14–7.11 (m, 2H), 6.81 (td, J = 8.5, 0.9 Hz, 1H), 2.22 (s, 3H) ppm. ^{13}C NMR (126 MHz, CDCl_3) δ 158.49 (ddd, J = 249.9, 12.8, 5.7 Hz), 136.49, 134.57, 134.56, 133.20 (dd, J = 9.5, 7.1 Hz), 131.96, 129.69, 125.74, 121.03 (dd, J = 17.6, 3.8 Hz), 116.38, 110.95 (dd, J = 21.2, 3.9 Hz), 104.53 (t, J = 20.1 Hz), 14.10 (d, J = 3.2 Hz) ppm. IR (KBr) ν 3121, 3096, 2924, 2852, 1497, 1482, 1265, 1093, 958 cm^{-1} . HRMS (ES^+) calculated for $\text{C}_{16}\text{H}_{11}\text{Cl}_2\text{F}_2\text{N}_2$ [$\text{M} + \text{H}$] $^+$ 339.0267, found 339.0269.

2-Chloro-1-(4-chlorophenyl)-5-(2,6-difluoro-3-methylphenyl)-1H-imidazole (63). Following synthetic procedure E using 1-(4-chlorophenyl)-5-(2,6-difluoro-3-methylphenyl)-1H-imidazole (0.326 g, 1.07 mmol), purification by silica gel column chromatography (hexanes/EtOAc 100:0 to 80:20) afforded the title compound as a brown solid (0.030 g, 0.088 mmol, 8% yield). ^1H NMR (500 MHz, CDCl_3) δ 7.35–7.32 (m, 2H), 7.16 (s, 1H), 7.14–7.08 (m, 3H), 6.71 (td, J = 8.5, 1.1 Hz, 1H), 2.15 (s, 3H) ppm. ^{13}C NMR (126 MHz, CDCl_3) δ 158.66 (ddd, J = 248.9, 13.9, 5.4 Hz), 135.30, 134.12, 133.71, 132.66 (t, J = 8.2 Hz), 130.33, 129.48, 128.68, 123.01, 120.95 (dd, J = 18.0, 4.0 Hz), 110.88 (dd, J = 21.7, 3.8 Hz), 106.33 (t, J = 20.1 Hz), 14.27 (d, J = 3.1 Hz) ppm. IR (KBr) ν 3445, 2919, 2848, 1496, 1478, 1443, 1093, 1042 cm^{-1} . HRMS (ES^+) calculated for $\text{C}_{16}\text{H}_{11}\text{Cl}_2\text{F}_2\text{N}_2$ [$\text{M} + \text{H}$] $^+$ 339.0267, found 339.0257.

4-Chloro-5-(3-chloro-2,6-difluorophenyl)-1-(4-chlorophenyl)-1H-imidazole (64). Following synthetic procedure E using 5-(3-chloro-2,6-difluorophenyl)-1-(4-chlorophenyl)-1H-imidazole (0.280 g, 0.434 mmol, 0.861 mmol), purification by silica gel column chromatography (hexanes/EtOAc 100:0 to 80:20) afforded the title compound as a yellow solid (0.156 g, 0.434 mmol, 50% yield). ^1H NMR (500 MHz, CDCl_3) δ 7.69 (s, 1H), 7.41 (td, J = 8.6, 5.6 Hz, 1H), 7.34–7.31 (m, 2H), 7.09 (m, 2H), 6.88–6.84 (m, 1H) ppm. ^{13}C NMR (126 MHz, CDCl_3) δ 158.79 (dd, J = 252.6, 4.4 Hz), 155.89 (dd, J = 253.6, 6.2 Hz), 137.09, 135.05, 134.27, 132.65, 132.28 (d, J = 9.6 Hz), 129.97, 125.85, 117.26 (dd, J = 18.4, 4.1 Hz), 115.25, 112.37 (dd, J = 23.3, 4.2 Hz), 106.79 (t, J = 20.1 Hz) ppm. IR (KBr) ν 3121, 3104, 3075, 2932, 2848, 1558, 1497, 1472, 1453, 1267, 1092 cm^{-1} . HRMS (ES^+) calculated for $\text{C}_{15}\text{H}_8\text{Cl}_3\text{F}_2\text{N}_2$ [$\text{M} + \text{H}$] $^+$ 358.9721, found 358.9724.

4-Chloro-5-(3-chloro-2,6-difluorophenyl)-1-(4-chlorophenyl)-2-methyl-1H-imidazole (65). Following synthetic procedure F using 4-chloro-5-(3-chloro-2,6-difluorophenyl)-1-(4-chlorophenyl)-1H-imidazole (0.078 g, 0.216 mmol), purification by silica gel column chromatography (hexanes/EtOAc 100:0 to 80:20) afforded the title compound as a brown solid (0.039 g, 0.104 mmol, 48% yield). ^1H NMR (500 MHz, CDCl_3) δ 7.38–7.33 (m, 3H), 7.07 (d, J = 8.6 Hz, 2H), 6.83–6.79 (m, 1H), 2.30 (s, 3H) ppm. ^{13}C NMR (126 MHz, CDCl_3) δ 159.02 (dd, J = 251.5, 4.4 Hz), 156.10 (dd, J = 252.9, 6.3 Hz), 146.08, 135.50, 134.14, 132.05 (d, J = 9.6 Hz), 130.54, 129.91, 128.29, 117.08 (dd, J = 18.5, 4.1 Hz), 115.24, 112.19 (dd, J = 23.5, 4.4 Hz), 107.42 (t, J = 20.5 Hz), 14.06 ppm. IR (KBr) ν 3100, 3071, 2928, 2848, 1558, 1495, 1465, 1399, 1495, 1465, 1399, 1338, 1287, 1242, 1219, 1092, 1011, 997 cm^{-1} . HRMS (ES^+) calculated for $\text{C}_{16}\text{H}_{10}\text{Cl}_3\text{F}_2\text{N}_2$ [$\text{M} + \text{H}$] $^+$ 372.9878, found 372.9864.

2-Chloro-5-(3-chloro-2,6-difluorophenyl)-1-(4-chlorophenyl)-1H-imidazole (66). Following synthetic procedure E using 5-(3-chloro-2,6-difluorophenyl)-1-(4-chlorophenyl)-1H-imidazole (0.280 g, 0.861 mmol), purification by silica gel column chromatography (hexanes/EtOAc 100:0 to 80:20) afforded the title compound as a yellow solid (0.050 g, 0.139 mmol, 16% yield). ^1H NMR (500 MHz, CDCl_3) δ 7.37–7.32 (m, 3H), 7.20 (s, 1H), 7.14–7.11 (m, 2H), 6.80 (td, J = 8.6, 1.4 Hz, 1H) ppm. ^{13}C NMR (126 MHz, CDCl_3) δ 158.83 (dd, J = 251.3, 4.1 Hz), 155.97 (dd, J = 252.5, 6.2 Hz), 135.64, 134.85,

4-Chloro-1-(4-chlorophenyl)-5-(4-fluorophenyl)-1H-imidazole (76). Following synthetic procedure E using 1-(4-chlorophenyl)-5-(4-fluorophenyl)-1H-imidazole (0.124 g, 0.455 mmol), purification by silica gel column chromatography (hexanes/EtOAc 100:0 to 80:20) afforded the title compound as a white solid (0.060 g, 0.195 mmol, 43% yield). ¹H NMR (500 MHz, CDCl₃) δ 7.57 (s, 1H), 7.36–7.33 (m, 2H), 7.18–7.15 (m, 2H), 7.06–6.99 (m, 4H) ppm. ¹³C NMR (126 MHz, CDCl₃) δ 162.58 (d, J = 249.6 Hz), 135.74, 134.73 (d, J = 3.7 Hz), 131.66 (d, J = 8.2 Hz), 129.99, 129.33, 126.66, 126.23, 123.39 (d, J = 3.4 Hz), 115.96, 115.78 ppm. IR (KBr) ν 3117, 3062, 2962, 2916, 2848, 1683, 1652, 1599, 1575, 1558, 1497 cm⁻¹. HRMS (ES⁺) calculated for C₁₅H₁₀Cl₂FN₂ [M + H]⁺ 307.0205, found 307.0206.

2-Chloro-1-(4-chloro-2-fluorophenyl)-5-(2,6-difluorophenyl)-1H-imidazole (77). Following synthetic procedure E using 1-(4-chloro-2-fluorophenyl)-5-(2,6-difluorophenyl)-1H-imidazole (0.351 g, 1.14 mmol), purification by silica gel column chromatography (hexanes/EtOAc 100:0 to 80:20) afforded the title compound as a yellow solid (0.025 g, 0.073 mmol, 6% yield). ¹H NMR (500 MHz, CDCl₃) δ 7.31–7.26 (m, 1H), 7.22 (s, 1H), 7.19 (d, J = 9.3 Hz, 1H), 7.15 (d, J = 3.1 Hz, 2H), 6.85 (t, J = 7.6 Hz, 2H) ppm. ¹³C NMR (126 MHz, CDCl₃) δ 160.60 (dd, J = 251.4, 5.9 Hz), 157.37 (d, J = 257.9 Hz), 136.78 (d, J = 9.2 Hz), 134.86, 131.52 (t, J = 10.3 Hz), 130.78, 130.32, 125.13, 125.10, 122.95, 121.74 (d, J = 13.0 Hz), 117.73 (d, J = 23.1 Hz), 111.69 (dd, J = 20.5, 5.0 Hz), 106.50 (t, J = 19.5 Hz) ppm. IR (KBr) ν 3104, 3071, 2936, 2860, 1683, 1652, 1634, 1587, 1558, 1538, 1505 cm⁻¹. HRMS (ES⁺) calculated for C₁₅H₈Cl₂F₃N₂ [M + H]⁺ 343.0017, found 343.0013.

4-Chloro-1-(4-chloro-2-fluorophenyl)-5-(2,6-difluorophenyl)-1H-imidazole (78). Following synthetic procedure E using 1-(4-chloro-2-fluorophenyl)-5-(2,6-difluorophenyl)-1H-imidazole (0.351 g, 1.14 mmol), purification by silica gel column chromatography (hexanes/EtOAc 100:0 to 80:20) afforded the title compound as a yellow solid (0.126 g, 0.367 mmol, 32% yield). ¹H NMR (500 MHz, CDCl₃) δ 7.65 (s, 1H), 7.38–7.33 (m, 1H), 7.19–7.17 (m, 1H), 7.13 (q, J = 6.4 Hz, 2H), 6.90 (t, J = 7.8 Hz, 2H) ppm. ¹³C NMR (126 MHz, CDCl₃) δ 160.74 (dd, J = 252.5, 5.9 Hz), 156.36 (d, J = 256.9 Hz), 137.49, 136.16 (d, J = 9.2 Hz), 132.18, 132.13 (t, J = 10.1 Hz), 128.61, 125.34 (d, J = 3.7 Hz), 122.69 (d, J = 12.6 Hz), 117.87 (d, J = 22.8 Hz), 116.88, 111.80 (dd, J = 20.6, 4.5 Hz), 105.04 (t, J = 19.6 Hz) ppm. IR (KBr) ν 3105, 2932, 1683, 1652, 1634, 1590, 1568, 1506 cm⁻¹. HRMS (ES⁺) calculated for C₁₅H₈Cl₂F₃N₂ [M + H]⁺ 343.0017, found 343.0018.

2-Chloro-1-(4-chlorophenyl)-5-(2,5-difluorophenyl)-1H-imidazole (79). Following synthetic procedure E using 1-(4-chlorophenyl)-5-(2,5-difluorophenyl)-1H-imidazole (0.300 g, 1.03 mmol), purification by silica gel column chromatography (hexanes/EtOAc 100:0 to 50:50) afforded the title compound as a yellow solid (0.010 g, 0.031 mmol, 3% yield). ¹H NMR (500 MHz, CDCl₃) δ 7.41–7.38 (m, 2H), 7.22 (s, 1H), 7.15–7.12 (m, 2H), 6.98–6.94 (m, 2H), 6.81–6.77 (m, 1H) ppm. ¹³C NMR (126 MHz, CDCl₃) δ 158.39 (dd, J = 245.6, 4.0 Hz), 155.71 (dd, J = 247.1, 3.7 Hz), 135.57, 134.62, 133.73, 129.79, 129.68 (d, J = 2.8 Hz), 128.87, 128.49, 118.43 (dd, J = 16.0, 10.3 Hz), 117.45–116.90 (m) ppm. IR (KBr) ν 3071, 2932, 2857, 1495 cm⁻¹. HRMS (ES⁺) calculated for C₁₅H₉Cl₂F₂N₂ [M + H]⁺ 325.0111, found 325.0110.

4-Chloro-1-(4-chlorophenyl)-5-(2,5-difluorophenyl)-1H-imidazole (80). Following synthetic procedure E using 1-(4-chlorophenyl)-5-(2,5-difluorophenyl)-1H-imidazole (0.300 g, 1.03 mmol), purification by silica gel column chromatography (hexanes/EtOAc 100:0 to 50:50) afforded the title compound as a yellow solid (0.030 g, 0.092 mmol, 9% yield). ¹H NMR (500 MHz, CDCl₃) δ 7.64 (s, 1H), 7.35–7.33 (m, 2H), 7.10–7.03 (m, 4H), 6.96 (td, J = 8.8, 4.5 Hz, 1H) ppm. ¹³C NMR (126 MHz, CDCl₃) δ 158.48 (dd, J = 244.1, 2.0 Hz), 155.77 (dd, J = 246.1, 1.7 Hz), 144.02, 136.41, 134.84, 134.79, 131.12, 129.97, 129.80, 129.45, 127.34, 125.83, 123.07, 121.05, 118.61 (dd, J = 24.9, 2.7 Hz), 117.94 (dd, J = 24.0, 8.5 Hz), 117.36 (dd, J = 24.5, 8.9 Hz), 116.91 (dd, J = 18.1, 9.0 Hz) ppm. IR (KBr) ν 3126, 3100, 3067, 2924, 2857, 1733, 1683, 1652, 1558, 1539, 1497 cm⁻¹. HRMS (ES⁺) calculated for C₁₅H₉Cl₂F₂N₂ [M + H]⁺ 325.0111, found 325.0095.

4-Chloro-5-(2,6-difluorophenyl)-1-(4-(trifluoromethoxy)phenyl)-1H-imidazole (81). Following synthetic procedure E using 5-(2,6-difluorophenyl)-1-(4-(trifluoromethoxy)phenyl)-1H-imidazole (0.400 g,

1.17 mmol), purification by silica gel column chromatography (hexanes/EtOAc 85:15) afforded the title compound as a white solid (0.192 g, 0.512 mmol, 44% yield). ¹H NMR (500 MHz, CDCl₃) δ 7.70 (s, 1H), 7.43–7.33 (m, 1H), 7.24–7.16 (m, 4H), 6.91 (t, J = 7.8 Hz, 2H) ppm. ¹³C NMR (126 MHz, CDCl₃) δ 160.71 (dd, J = 252.1, 6.0 Hz), 149.23–149.16 (m), 136.84, 134.52, 132.53, 132.20 (t, J = 10.2 Hz), 126.25, 122.01, 120.39 (q, J = 238.7 Hz), 116.18, 111.88 (dd, J = 20.5, 5.1 Hz), 105.32 (t, J = 19.7 Hz) ppm. IR (KBr) ν 3121, 3088, 1632, 1588, 1565, 1513, 1473, 1330, 1259, 1212, 1169, 1099 cm⁻¹. HRMS (ES⁺) calculated for C₁₆H₉ClF₅N₂O [M + H]⁺ 375.0324, found 375.0334.

2-Chloro-5-(2,6-difluorophenyl)-1-(4-(trifluoromethoxy)phenyl)-1H-imidazole (82). Following synthetic procedure E using 5-(2,6-difluorophenyl)-1-(4-(trifluoromethoxy)phenyl)-1H-imidazole (0.400 g, 1.17 mmol), purification by silica gel column chromatography (hexanes/EtOAc 85:15) afforded the title compound as a white solid (0.033 g, 0.088 mmol, 8% yield). ¹H NMR (500 MHz, CDCl₃) δ 7.34–7.25 (m, 1H), 7.27–7.20 (m, 4H), 7.20 (s, 1H), 6.88–6.82 (m, 2H) ppm. ¹³C NMR (126 MHz, CDCl₃) δ 160.59 (dd, J = 251.3, 5.8 Hz), 149.51–149.44 (m), 134.36, 133.35, 131.57 (t, J = 10.2 Hz), 130.53, 128.96, 122.52, 121.41, 120.39 (q, J = 259.6 Hz), 111.67 (dd, J = 21.2, 4.6 Hz), 106.84 (t, J = 19.5 Hz) ppm. IR (KBr) ν 3077, 2920, 2852, 1632, 1586, 1511, 1469, 1436, 1388, 1261, 1211, 1172, 1001 cm⁻¹. HRMS (ES⁺) calculated for C₁₆H₈ClF₅N₂NaO [M + Na]⁺ 397.0143, found 397.0149.

2,4-Dichloro-5-(2,6-difluorophenyl)-1-(4-(trifluoromethoxy)phenyl)-1H-imidazole (83). Following synthetic procedure E using 5-(2,6-difluorophenyl)-1-(4-(trifluoromethoxy)phenyl)-1H-imidazole (0.400 g, 1.17 mmol), purification by silica gel column chromatography (hexanes/EtOAc 85:15) afforded the title compound as a white solid (0.028 g, 0.068 mmol, 6% yield). ¹H NMR (500 MHz, CDCl₃) δ 7.40–7.30 (m, 1H), 7.27–7.19 (m, 4H), 6.91–6.84 (m, 2H) ppm. ¹³C NMR (126 MHz, CDCl₃) δ 160.74 (dd, J = 252.3, 5.6 Hz), 149.85–149.77 (m), 132.76, 132.65, 132.61 (t, J = 10.3 Hz), 130.50, 128.96, 121.54, 120.34 (q, J = 258.7 Hz), 118.60, 111.81 (dd, J = 21.0, 4.3 Hz), 104.93 (t, J = 19.4 Hz) ppm. IR (KBr) ν 3079, 2921, 2851, 1633, 1590, 1570, 1511, 1468, 1439, 1388, 1263, 1213, 1174 cm⁻¹. HRMS (ES⁺) calculated for C₁₆H₈Cl₂F₅N₂O [M + H]⁺ 408.9934, found 408.9940.

4-Chloro-1-(4-chlorophenyl)-5-(2,6-difluorophenyl)-1H-imidazole (84). Following synthetic procedure E using 1-(4-chlorophenyl)-5-(2,6-difluorophenyl)-1H-imidazole (0.400 g, 1.38 mmol), purification by silica gel column chromatography (hexanes/EtOAc 85:15) afforded the title compound as a white solid (0.265 g, 0.815 mmol, 59% yield). ¹H NMR (500 MHz, CDCl₃) δ 7.69 (s, 1H), 7.41–7.35 (m, 1H), 7.33 (d, J = 8.0 Hz, 2H), 7.12–7.05 (m, 2H), 6.91 (t, J = 7.9 Hz, 2H) ppm. ¹³C NMR (126 MHz, CDCl₃) δ 160.67 (dd, J = 252.0, 5.9 Hz), 136.75, 134.89, 134.65, 132.40, 132.12 (t, J = 10.1 Hz), 129.91, 125.93, 116.10, 111.88 (dd, J = 21.1, 4.3 Hz), 105.36 (t, J = 19.5 Hz) ppm. IR (KBr) ν 3128, 2917, 2849, 1631, 1587, 1564, 1497, 1470, 1453, 1383, 1265, 1236, 1091, 998 cm⁻¹. HRMS (ES⁺) calculated for C₁₅H₉Cl₂F₂N₂ [M + H]⁺ 325.0111, found 325.0122.

4-Chloro-1-(4-chlorophenyl)-5-(2,6-difluorophenyl)-2-methyl-1H-imidazole (85). Following synthetic procedure F using 4-chloro-1-(4-chlorophenyl)-5-(2,6-difluorophenyl)-1H-imidazole (0.050 g, 0.154 mmol), purification by silica gel column chromatography (hexanes/EtOAc 80:20) afforded the title compound as a white solid (0.020 g, 0.059 mmol, 38% yield). ¹H NMR (500 MHz, CDCl₃) δ 7.37–7.31 (m, 2H), 7.31–7.27 (m, 1H), 7.08 (d, J = 8.6 Hz, 2H), 6.89–6.82 (m, 2H), 2.31 (s, 3H) ppm. ¹³C NMR (126 MHz, CDCl₃) δ 160.83 (dd, J = 250.5, 6.9 Hz), 145.60, 135.23, 134.48, 131.79 (t, J = 10.1 Hz), 130.20, 129.75, 128.37, 116.02, 111.63 (dd, J = 20.4, 4.8 Hz), 105.96 (t, J = 17.7 Hz), 14.13 ppm. IR (KBr) ν 3064, 2960, 2921, 2850, 1634, 1576, 1494, 1467, 1402, 1278, 1238, 1093, 999 cm⁻¹. HRMS (ES⁺) calculated for C₁₆H₁₁Cl₂F₂N₂ [M + H]⁺ 339.0267, found 339.0265.

4-Chloro-1-(4-chlorophenyl)-5-(2,6-difluorophenyl)-2-ethyl-1H-imidazole (86). Following synthetic procedure F using 4-chloro-1-(4-chlorophenyl)-5-(2,6-difluorophenyl)-1H-imidazole (0.040 g, 0.123 mmol), purification by silica gel column chromatography (hexanes/EtOAc 85:15) afforded the title compound as a white solid (0.015 g, 0.042 mmol, 35% yield). ¹H NMR (500 MHz, CDCl₃) δ 7.36–7.30 (m, 2H), 7.30–7.27

5.0 Hz, 1H), 6.80–6.72 (m, 1H), 3.82 (s, 3H) ppm. ^{13}C NMR (126 MHz, CDCl_3) δ 153.85 (dd, $J = 243.6, 4.2$ Hz), 149.92 (dd, $J = 250.9, 5.9$ Hz), 144.38 (dd, $J = 11.0, 3.4$ Hz), 135.36, 134.38, 133.55, 130.48, 129.57, 128.66, 122.51, 114.40 (dd, $J = 9.5, 3.2$ Hz), 110.34 (dd, $J = 23.3, 4.4$ Hz), 107.70 (dd, $J = 21.2, 16.9$ Hz), 56.84 ppm. IR (KBr) ν 3096, 2923, 2849, 1590, 1493, 1459, 1438, 1383, 1318, 1244, 1175, 1123, 1093, 1058 cm^{-1} . HRMS (ES^+) calculated for $\text{C}_{16}\text{H}_{11}\text{Cl}_2\text{F}_2\text{N}_2\text{O}$ [$\text{M} + \text{H}$] $^+$ 355.0217, found 355.0219.

2,4-Dichloro-1-(4-chlorophenyl)-5-(2,6-difluoro-3-methoxyphenyl)-1H-imidazole (97). Following synthetic procedure E using 1-(4-chlorophenyl)-5-(2,6-difluoro-3-methoxyphenyl)-1H-imidazole (0.132 g, 0.412 mmol), purification by silica gel column chromatography (hexanes/EtOAc 80:20) afforded the title compound as a yellow solid (0.009 g, 0.023 mmol, 6% yield). ^1H NMR (500 MHz, CDCl_3) δ 7.37–7.34 (m, 2H), 7.15–7.12 (m, 2H), 6.94 (td, $J = 9.2, 5.0$ Hz, 1H), 6.81–6.77 (m, 1H), 3.83 (s, 3H) ppm. ^{13}C NMR (126 MHz, CDCl_3) δ 153.94 (dd, $J = 244.9, 4.0$ Hz), 150.12 (dd, $J = 252.5, 5.6$ Hz), 144.45 (dd, $J = 10.6, 3.4$ Hz), 135.95, 133.06, 132.65, 130.49, 129.78, 128.61, 118.59, 115.43 (dd, $J = 9.8, 3.0$ Hz), 110.51 (dd, $J = 22.8, 4.3$ Hz), 105.84 (dd, $J = 21.4, 16.8$ Hz), 56.88 ppm. IR (KBr) ν 2921, 2850, 1639, 1494, 1440, 1384, 1331, 1251, 1090 cm^{-1} . HRMS (ES^+) calculated for $\text{C}_{16}\text{H}_{10}\text{Cl}_3\text{F}_2\text{N}_2\text{O}$ [$\text{M} + \text{H}$] $^+$ 388.9827, found 388.9832.

4-Chloro-1-(4-chlorophenyl)-5-phenyl-1H-imidazole (98). Following synthetic procedure E using 1-(4-chlorophenyl)-5-phenyl-1H-imidazole (0.070 g, 0.275 mmol), purification by silica gel column chromatography (hexanes/EtOAc 80:20) afforded the title compound as a yellow solid (0.061 g, 0.211 mmol, 77% yield). X-ray quality crystals were obtained by slow evaporation from a CH_2Cl_2 /hexanes solution (see Supporting Information): mp (CH_2Cl_2 /hexanes) 126–128 $^\circ\text{C}$. ^1H NMR (500 MHz, CDCl_3) δ 7.58 (s, 1H), 7.36–7.29 (m, 5H), 7.22–7.16 (m, 2H), 7.09–7.02 (m, 2H) ppm. ^{13}C NMR (126 MHz, CDCl_3) δ 135.72, 134.91, 134.49, 129.89, 129.75, 129.24, 128.62, 128.44, 127.28, 127.09, 126.61 ppm. IR (KBr) ν 3121, 3096, 3034, 2917, 2849, 1607, 1558, 1497, 1483, 1467, 1413, 1329, 1259, 1199, 1090 cm^{-1} . HRMS (ES^+) calculated for $\text{C}_{15}\text{H}_{11}\text{Cl}_2\text{N}_2$ [$\text{M} + \text{H}$] $^+$ 289.0299, found 289.0300.

2-Chloro-1-(4-chlorophenyl)-5-phenyl-1H-imidazole (99). Following synthetic procedure E using 1-(4-chlorophenyl)-5-phenyl-1H-imidazole (0.070 g, 0.275 mmol), purification by silica gel column chromatography (hexanes/EtOAc 80:20) afforded the title compound as a yellow solid (0.007 g, 0.025 mmol, 9% yield). ^1H NMR (500 MHz, CDCl_3) δ 7.45–7.38 (m, 2H), 7.27–7.22 (m, 3H), 7.20–7.12 (m, 3H), 7.10–7.03 (m, 2H) ppm. ^{13}C NMR (126 MHz, CDCl_3) δ 135.32, 134.09, 133.77, 129.85, 129.37, 128.95, 128.76, 128.12, 127.94, 127.21, 125.13 ppm. IR (KBr) ν 2956, 2918, 2850, 1487, 1457, 1432, 1383, 1307, 1256, 1146, 1146, 1093 cm^{-1} . HRMS (ES^+) calculated for $\text{C}_{15}\text{H}_{11}\text{Cl}_2\text{N}_2$ [$\text{M} + \text{H}$] $^+$ 289.0299, found 289.0324.

2,4-Dichloro-1-(4-chlorophenyl)-5-phenyl-1H-imidazole (100). Following synthetic procedure E using 1-(4-chlorophenyl)-5-phenyl-1H-imidazole (0.070 g, 0.275 mmol), purification by silica gel column chromatography (hexanes/EtOAc 80:20) afforded the title compound as a yellow solid (0.008 g, 0.024 mmol, 9% yield). ^1H NMR (500 MHz, CDCl_3) δ 7.40–7.36 (m, 2H), 7.30–7.27 (m, 3H), 7.16–7.12 (m, 2H), 7.12–7.08 (m, 2H) ppm. ^{13}C NMR (126 MHz, CDCl_3) δ 135.64, 133.57, 131.34, 129.89, 129.59, 129.21, 128.71, 128.65, 127.20, 127.05 ppm. IR (KBr) ν 2956, 2917, 2849, 1493, 1452, 1381, 1230, 1091 cm^{-1} . HRMS (ES^+) calculated for $\text{C}_{15}\text{H}_{10}\text{Cl}_3\text{N}_2$ [$\text{M} + \text{H}$] $^+$ 322.9910, found 322.9906.

4-Chloro-1-(4-chlorophenyl)-5-(4-methoxyphenyl)-1H-imidazole (101). Following synthetic procedure E using 1-(4-chlorophenyl)-5-(4-methoxyphenyl)-1H-imidazole (0.220 g, 0.773 mmol), purification by silica gel column chromatography (hexanes/EtOAc 80:20) afforded the title compound as a yellow solid (0.159 g, 0.498 mmol, 65% yield). ^1H NMR (500 MHz, CDCl_3) δ 7.55 (s, 1H), 7.36–7.31 (m, 2H), 7.11 (d, $J = 8.1$ Hz, 2H), 7.06 (d, $J = 7.9$ Hz, 2H), 6.84 (d, $J = 8.3$ Hz, 2H), 3.79 (s, 3H) ppm. ^{13}C NMR (126 MHz, CDCl_3) δ 159.66, 135.29, 135.02, 134.43, 131.15, 129.87, 128.71, 127.05, 126.64, 119.49, 114.17, 55.36 ppm. IR (KBr) ν 3116, 3004, 2960, 2836, 1713, 1614, 1556, 1497, 1467, 1290, 1253, 1179, 1087 cm^{-1} . HRMS (ES^+) calculated for $\text{C}_{16}\text{H}_{12}\text{Cl}_2\text{N}_2\text{NaO}$ [$\text{M} + \text{Na}$] $^+$ 341.0224, found 341.0229.

4-Chloro-1-(2-chlorophenyl)-5-(2,6-difluorophenyl)-1H-imidazole (102). Following synthetic procedure E using 1-(2-chlorophenyl)-5-(2,6-difluorophenyl)-1H-imidazole (0.260 g, 0.894 mmol), purification by silica gel column chromatography (hexanes/EtOAc 75:25) afforded the title compound as a white solid (0.187 g, 0.575 mmol, 64% yield). ^1H NMR (500 MHz, CDCl_3) δ 7.63 (s, 1H), 7.42 (d, $J = 7.9$ Hz, 1H), 7.36–7.29 (m, 2H), 7.29–7.26 (m, 2H), 6.85 (t, $J = 8.6$ Hz, 2H) ppm. ^{13}C NMR (126 MHz, CDCl_3) δ 160.77 (dd, $J = 252.5, 5.9$ Hz), 137.58, 133.55, 131.88 (t, $J = 10.2$ Hz), 131.70, 131.67, 130.73, 130.61, 129.10, 127.60, 117.02, 111.64 (dd, $J = 21.8, 3.6$ Hz), 105.35 (t, $J = 19.5$ Hz) ppm. IR (KBr) ν 3129, 3052, 2988, 2922, 2846, 1633, 1589, 1568, 1492, 1471, 1455, 1266, 1238, 1003 cm^{-1} . HRMS (ES^+) calculated for $\text{C}_{15}\text{H}_9\text{Cl}_2\text{F}_2\text{N}_2$ [$\text{M} + \text{H}$] $^+$ 325.0111, found 325.0111.

2-Chloro-1-(2-chlorophenyl)-5-(2,6-difluorophenyl)-1H-imidazole (103). Following synthetic procedure E using 1-(2-chlorophenyl)-5-(2,6-difluorophenyl)-1H-imidazole (0.260 g, 0.894 mmol), purification by silica gel column chromatography (hexanes/EtOAc 75:25) afforded the title compound as a white solid (0.026 g, 0.080 mmol, 9% yield). ^1H NMR (500 MHz, CDCl_3) δ 7.40 (d, $J = 8.0$ Hz, 1H), 7.36–7.27 (m, 3H), 7.25–7.16 (m, 2H), 6.79 (t, $J = 7.7$ Hz, 2H) ppm. ^{13}C NMR (126 MHz, CDCl_3) δ 160.72 (dd, $J = 251.5, 5.8$ Hz), 134.75, 133.21, 132.81, 131.34 (t, $J = 10.2$ Hz), 131.06, 130.51, 130.44, 130.32, 127.44, 122.84, 111.53 (dd, $J = 20.6, 5.1$ Hz), 106.87 (t, $J = 19.5$ Hz) ppm. IR (KBr) ν 2916, 2852, 1633, 1587, 1487, 1468, 1435, 1383, 1313, 1277, 1235, 1000 cm^{-1} . HRMS (ES^+) calculated for $\text{C}_{15}\text{H}_9\text{Cl}_2\text{F}_2\text{N}_2$ [$\text{M} + \text{H}$] $^+$ 325.0111, found 325.0119.

2,4-Dichloro-1-(2-chlorophenyl)-5-(2,6-difluorophenyl)-1H-imidazole (104). Following synthetic procedure E using 4-chloro-1-(2-chlorophenyl)-5-(2,6-difluorophenyl)-1H-imidazole (0.060 g, 0.184 mmol), purification by silica gel column chromatography (hexanes/EtOAc 80:20) afforded the title compound as a white solid (0.047 g, 0.131 mmol, 71% yield). ^1H NMR (500 MHz, CDCl_3) δ 7.44 (d, $J = 7.9$ Hz, 1H), 7.40–7.27 (m, 4H), 6.88 (t, $J = 8.5$ Hz, 1H), 6.82 (t, $J = 8.6$ Hz, 1H) ppm. ^{13}C NMR (126 MHz, CDCl_3) δ 161.07 (dd, $J = 254.4, 5.9$ Hz), 133.11, 133.08, 132.37 (t, $J = 11.2$ Hz), 131.53, 130.56, 130.39, 130.24, 130.22, 127.62, 118.89, 111.95 (dd, $J = 21.7, 3.5$ Hz), 111.41 (dd, $J = 21.8, 3.7$ Hz), 104.92 (t, $J = 19.8$ Hz) ppm. IR (KBr) ν 3073, 2918, 2853, 1633, 1588, 1487, 1466, 1439, 1384, 1278, 1237, 1002 cm^{-1} . HRMS (ES^+) calculated for $\text{C}_{15}\text{H}_8\text{Cl}_3\text{F}_2\text{N}_2$ [$\text{M} + \text{H}$] $^+$ 358.9721, found 358.9717.

Acetyl-Tubulin Assay. QBI-293 cells (ATCC, Manassas, VA, USA) were maintained in Dulbecco's Modified Eagle's Medium (Mediatech Inc., Manassas, VA, USA) containing 10% fetal bovine serum (FBS) (Atlanta Biologicals, Lawrenceville, GA, USA), 2 mM L-glutamine (Mediatech), 50 units/mL penicillin, and 50 $\mu\text{g}/\text{mL}$ streptomycin (1% penicillin/streptomycin; Thermo Fisher Scientific, Waltham, MA, USA). Cells were maintained at 37 $^\circ\text{C}$ in a humidified atmosphere (5% CO_2) for all experiments. For compound testing, cells were dissociated with trypsin/EDTA (Thermo Fisher Scientific) and plated at 6×10^5 cells/well in 6-well plates. The medium was aspirated after overnight incubation and fresh medium containing vehicle or test compound was added. After incubating for 4 h, cells were washed once with 1 \times phosphate-buffered saline (PBS), pH 7.4 and then lysed in 200 μL RIPA buffer containing protease inhibitor cocktail, 1 mM PMSF, and 1 μM TSA. Lysed cells were scraped into 1.5 mL Beckman ultracentrifuge tubes (Beckman, Brea, CA, USA) and centrifuged at 100000g for 30 min at 4 $^\circ\text{C}$. Following centrifugation, the supernatant from each sample was collected and analyzed for protein content by BCA assay. The samples subsequently underwent analysis for acetyl-tubulin and α -tubulin levels by ELISA, as previously described.³⁹

RBL-1 Cell PG and LT Assay. Inhibition of PG and LT synthesis by test compounds was determined through the utilization of an established RBL-1 cell assay.⁴⁰ Briefly, RBL-1 cells (ATCC) were maintained in RPMI 1640 medium (Mediatech Inc., Manassas, VA) containing 10% fetal bovine serum (FBS) (Atlanta Biologicals, Lawrenceville, GA), 1 mM L-glutamine (Mediatech), 50 U/mL penicillin, and 0.05 mg/mL streptomycin (Thermo Fisher Scientific). For analysis of PG and LT production, RBL-1 cells were plated at a density of 9×10^5 cells/well in 24-well plates. After 2 h incubation at

37 °C, cells were added with indicated concentrations of test compounds. Following 2 h incubation with test compounds, cells were incubated with 12 μM calcium ionophore, A23187, for 15 min to induce arachidonic acid production. Cell culture supernatants (200 μL/well) were then collected and treated with 600 μL of MeOH containing 0.01% BHT (butylated hydroxytoluene) to extract eicosanoids. After centrifugation, the supernatant was dried with a vacuum centrifugation and redissolved in 200 μL of 50% acetonitrile. Enzyme products were quantified with an Acquity UPLC-TQ MS system (Waters Corporation, Milford, MA). Injections (10 μL) were separated on an Acquity BEH C18, 1.7 μm, 2.1 mm × 50 mm column at 37 °C using a gradient from 5 to 95% acetonitrile with 10 mM ammonium formate over 2 min at 0.6 mL/min. Combined PGD₂+PGE₂, as well as LTB₄, were detected in negative ion mode using compound specific collision induced mass transitions (PGD₂ and PGE₂, 351 > 315; LTB₄, 335 > 195). To separate the isomeric prostaglandins PGD₂ and PGE₂, a higher resolution gradient from 5 to 60% acetonitrile over 3 min at 0.6 mL/min was used. The cysteinyl leukotriene LTC₄ was separated using a gradient from 5 to 95% acetonitrile with 0.1% formic acid over 2 min at 0.6 mL/min. LTC₄ was detected using electrospray ionization in positive mode while monitoring for a compound specific mass transition (626 > 189). Chromatograms are integrated and peak areas used to quantitate unknowns against a curve of standards (Cayman Chemical, Ann Arbor, MI) from 1 to 50 ng/mL in 50% acetonitrile.

Brain and Plasma Compound Determinations. All animal protocols were approved by the University of Pennsylvania Institutional Animal Care and Use Committee (IACUC). Test compounds were administered to groups of three 2–5 month old CD-1 or B6SJL mice, with both female and male mice used but not mixed within experimental groups. For standard single time-point brain and plasma determinations, mice were injected i.p. with a single dose of 5 mg/kg compound dissolved in DMSO, or a dose of 2 mg/kg if two or three compounds were dosed concurrently (cassette dosing). Compounds were quantified in plasma and brain homogenates as previously described.³⁹

■ ASSOCIATED CONTENT

Supporting Information

The Supporting Information is available free of charge on the ACS Publications website at DOI: 10.1021/acs.jmedchem.7b00475.

NMR spectra of test compounds; X-ray crystal structures of compound **98** (CCDC 1529316); details for the docking studies; analysis of Table 2 compounds for their ability to reduce multiple COX and 5-LOX products (PDF)

SMILES string structures along the full data set in tabular form (CSV)

Accession Codes

Authors will release the atomic coordinates and experimental data upon article publication.

■ AUTHOR INFORMATION

Corresponding Authors

*For C.B.: phone, 858-822-3663; E-mail, cballatore@ucsd.edu.

*For K.B.: phone, 215-615-5262; E-mail, kbrunden@upenn.edu.

ORCID

Amos B. Smith III: 0000-0002-1712-8567

Carlo Ballatore: 0000-0002-2718-3850

Notes

The authors declare no competing financial interest.

■ ACKNOWLEDGMENTS

Financial support for this work has been provided in part by NIH/NIA (grant AG044332-01), the Woods Charitable Foundation, and the Cenci Bolognetti Foundation (LM).

■ ABBREVIATIONS USED

TosMIC, toluenesulfonylmethyl isocyanide; LDA, lithium diisopropylamide; AcTub, acetylated α-tubulin

■ REFERENCES

- (1) Anighoro, A.; Bajorath, J.; Rastelli, G. Polypharmacology: challenges and opportunities in drug discovery. *J. Med. Chem.* **2014**, *57*, 7874–7887.
- (2) Geldenhuys, W. J.; Van der Schyf, C. J. Rationally designed multi-targeted agents against neurodegenerative diseases. *Curr. Med. Chem.* **2013**, *20*, 1662–1672.
- (3) Cavalli, A.; Bolognesi, M. L.; Minarini, A.; Rosini, M.; Tumiatti, V.; Recanatini, M.; Melchiorre, C. Multi-target-directed ligands to combat neurodegenerative diseases. *J. Med. Chem.* **2008**, *51*, 347–372.
- (4) Makani, V.; Zhang, B.; Han, H.; Yao, Y.; Lassalas, P.; Lou, K.; Paterson, I.; Lee, V. M. Y.; Trojanowski, J. Q.; Ballatore, C.; Smith, A. B., III; Brunden, K. R. Evaluation of the brain-penetrant microtubule-stabilizing agent, dictyostatin, in the PS19 tau transgenic mouse model of tauopathy. *Acta Neuropathol. Commun.* **2016**, *4*, 106.
- (5) Zhang, B.; Carroll, J.; Trojanowski, J. Q.; Yao, Y.; Iba, M.; Potuzak, J. S.; Hogan, A. M.; Xie, S. X.; Ballatore, C.; Smith, A. B., III; Lee, V. M.; Brunden, K. R. The microtubule-stabilizing agent, epothilone D, reduces axonal dysfunction, neurotoxicity, cognitive deficits, and Alzheimer-like pathology in an interventional study with aged tau transgenic mice. *J. Neurosci.* **2012**, *32*, 3601–3611.
- (6) Brunden, K. R.; Zhang, B.; Carroll, J.; Yao, Y.; Potuzak, J. S.; Hogan, A. M.; Iba, M.; James, M. J.; Xie, S. X.; Ballatore, C.; Smith, A. B., III; Lee, V. M.; Trojanowski, J. Q. Epothilone D improves microtubule density, axonal integrity, and cognition in a transgenic mouse model of tauopathy. *J. Neurosci.* **2010**, *30*, 13861–13866.
- (7) Barten, D. M.; Fanara, P.; Andorfer, C.; Hoque, N.; Wong, P. Y. A.; Husted, K. H.; Cadelina, G. W.; DeCarr, L. B.; Yang, L.; Liu, L.; Fessler, C.; Protassio, J.; Riff, T.; Turner, H.; Janus, C. G.; Sankaranarayanan, S.; Polson, C.; Meredith, J. E.; Gray, G.; Hanna, A.; Olson, R. E.; Kim, S. H.; Vite, G. D.; Lee, F. Y.; Albright, C. F. Hyperdynamic microtubules, cognitive deficits, and pathology are improved in tau transgenic mice with low doses of the microtubule-stabilizing agent BMS-241027. *J. Neurosci.* **2012**, *32*, 7137–7145.
- (8) Herbst-Robinson, K. J.; Liu, L.; James, M.; Yao, Y.; Xie, S. X.; Brunden, K. R. Inflammatory eicosanoids increase amyloid precursor protein expression via activation of multiple neuronal receptors. *Sci. Rep.* **2016**, *5*, 18286.
- (9) Montine, T. J.; Sidell, K. R.; Crews, B. C.; Markesbery, W. R.; Marnett, L. J.; Roberts, L. J., II; Morrow, J. D. Elevated CSF prostaglandin E2 levels in patients with probable AD. *Neurology* **1999**, *53*, 1495–1498.
- (10) Manev, H.; Chen, H.; Dzitoyeva, S.; Manev, R. Cyclooxygenases and 5-lipoxygenase in Alzheimer's disease. *Prog. Neuro-Psychopharmacol. Biol. Psychiatry* **2011**, *35*, 315–319.
- (11) Kitamura, Y.; Shimohama, S.; Koike, H.; Kakimura, J.; Matsuoka, Y.; Nomura, Y.; Gebicke-Haerter, P. J.; Taniguchi, T. Increased expression of cyclooxygenases and peroxisome proliferator-activated receptor-gamma in Alzheimer's disease brains. *Biochem. Biophys. Res. Commun.* **1999**, *254*, 582–586.
- (12) Fujimi, K.; Noda, K.; Sasaki, K.; Wakisaka, Y.; Tanizaki, Y.; Iida, M.; Kiyohara, Y.; Kanba, S.; Iwaki, T. Altered expression of COX-2 in subdivisions of the hippocampus during aging and in Alzheimer's disease: the Hisayama Study. *Dementia Geriatr. Cognit. Disord.* **2007**, *23*, 423–431.
- (13) Zhen, G.; Kim, Y. T.; Li, R. C.; Yocum, J.; Kapoor, N.; Langer, J.; Dobrowski, P.; Maruyama, T.; Narumiya, S.; Dore, S. PGE2 EP1 receptor exacerbated neurotoxicity in a mouse model of cerebral

ischemia and Alzheimer's disease. *Neurobiol. Aging* **2012**, *33*, 2215–2219.

(14) Liang, X.; Wang, Q.; Hand, T.; Wu, L.; Breyer, R. M.; Montine, T. J.; Andreasson, K. Deletion of the prostaglandin E2 EP2 receptor reduces oxidative damage and amyloid burden in a model of Alzheimer's disease. *J. Neurosci.* **2005**, *25*, 10180–10187.

(15) Shi, J.; Wang, Q.; Johansson, J. U.; Liang, X.; Woodling, N. S.; Priyam, P.; Loui, T. M.; Merchant, M.; Breyer, R. M.; Montine, T. J.; Andreasson, K. Inflammatory prostaglandin E2 signaling in a mouse model of Alzheimer disease. *Ann. Neurol.* **2012**, *72*, 788–798.

(16) Hoshino, T.; Namba, T.; Takehara, M.; Murao, N.; Matsushima, T.; Sugimoto, Y.; Narumiya, S.; Suzuki, T.; Mizushima, T. Improvement of cognitive function in Alzheimer's disease model mice by genetic and pharmacological inhibition of the EP(4) receptor. *J. Neurochem.* **2012**, *120*, 795–805.

(17) Woodling, N. S.; Wang, Q.; Priyam, P. G.; Larkin, P.; Shi, J.; Johansson, J. U.; Zagol-Ikapitte, I.; Boutaud, O.; Andreasson, K. I. Suppression of Alzheimer-associated inflammation by microglial prostaglandin-E2 EP4 receptor signaling. *J. Neurosci.* **2014**, *34*, 5882–5894.

(18) Firuzi, O.; Zhuo, J.; Chinnici, C. M.; Wisniewski, T.; Pratico, D. 5-Lipoxygenase gene disruption reduces amyloid-beta pathology in a mouse model of Alzheimer's disease. *FASEB J.* **2007**, *22*, 1169–1178.

(19) Ikonovic, M. D.; Abrahamson, E. E.; Uz, T.; Manev, H.; Dekosky, S. T. Increased 5-lipoxygenase immunoreactivity in the hippocampus of patients with Alzheimer's disease. *J. Histochem. Cytochem.* **2008**, *56*, 1065–1073.

(20) Chu, J.; Giannopoulos, P. F.; Ceballos-Diaz, C.; Golde, T. E.; Pratico, D. 5-Lipoxygenase gene transfer worsens memory, amyloid, and tau brain pathologies in a mouse model of Alzheimer disease. *Ann. Neurol.* **2012**, *72*, 442–454.

(21) Chu, J.; Pratico, D. Pharmacologic blockade of 5-lipoxygenase improves the amyloidotic phenotype of an Alzheimer's disease transgenic mouse model involvement of gamma-secretase. *Am. J. Pathol.* **2011**, *178*, 1762–1769.

(22) Hawkes, C. A.; Shaw, J. E.; Brown, M.; Sampson, A. P.; McLaurin, J.; Carare, R. O. MK886 reduces cerebral amyloid angiopathy severity in TgCRND8 mice. *Neurodegener. Dis.* **2014**, *13*, 17–23.

(23) Tang, S. S.; Wang, X. Y.; Hong, H.; Long, Y.; Li, Y. Q.; Xiang, G. Q.; Jiang, L. Y.; Zhang, H. T.; Liu, L. P.; Miao, M. X.; Hu, M.; Zhang, T. T.; Hu, W.; Ji, H.; Ye, F. Y. Leukotriene D4 induces cognitive impairment through enhancement of CysLT(1) R-mediated amyloid-beta generation in mice. *Neuropharmacology* **2013**, *65*, 182–192.

(24) Brunden, K. R.; Lee, V. M.; Smith, A. B.; Trojanowski, J. Q.; Ballatore, C. Altered microtubule dynamics in neurodegenerative disease: therapeutic potential of microtubule-stabilizing drugs. *Neurobiol. Dis.* **2017**, *2016*, 21.

(25) Phillis, J. W.; Horrocks, L. A.; Farooqui, A. A. Cyclooxygenases, lipoxygenases, and epoxygenases in CNS: their role and involvement in neurological disorders. *Brain Res. Rev.* **2006**, *52*, 201–243.

(26) Kang, K. H.; Liou, H. H.; Hour, M. J.; Liou, H. C.; Fu, W. M. Protection of dopaminergic neurons by 5-lipoxygenase inhibitor. *Neuropharmacology* **2013**, *73*, 380–387.

(27) Chou, V. P.; Holman, T. R.; Manning-Bog, A. B. Differential contribution of lipoxygenase isozymes to nigrostriatal vulnerability. *Neuroscience* **2013**, *228*, 73–82.

(28) Thakur, P.; Nehru, B. Anti-inflammatory properties rather than anti-oxidant capability is the major mechanism of neuroprotection by sodium salicylate in a chronic rotenone model of Parkinson's disease. *Neuroscience* **2013**, *231*, 420–431.

(29) Teismann, P. COX-2 in the neurodegenerative process of Parkinson's disease. *Biofactors* **2012**, *38*, 395–397.

(30) Yokota, O.; Terada, S.; Ishizu, H.; Ishihara, T.; Nakashima, H.; Kugo, A.; Tsuchiya, K.; Ikeda, K.; Hayabara, T.; Saito, Y.; Murayama, S.; Ueda, K.; Checler, F.; Kuroda, S. Increased expression of neuronal cyclooxygenase-2 in the hippocampus in amyotrophic lateral sclerosis both with and without dementia. *Acta Neuropathol.* **2004**, *107*, 399–405.

(31) Kong, W.; Hooper, K. M.; Ganea, D. The natural dual cyclooxygenase and 5-lipoxygenase inhibitor flavocoxid is protective in EAE through effects on Th1/Th17 differentiation and macrophage/microglia activation. *Brain, Behav., Immun.* **2016**, *53*, 59–71.

(32) Morphy, R.; Rankovic, Z.; Abraham, D. J. Medicinal chemistry approaches for multitarget drugs. In *Burger's Medicinal Chemistry and Drug Discovery*; John Wiley & Sons, Inc.: Hoboken, NJ, 2003; pp 249–274.

(33) Smith, C. J.; Zhang, Y.; Koboldt, C. M.; Muhammad, J.; Zweifel, B. S.; Shaffer, A.; Talley, J. J.; Masferrer, J. L.; Seibert, K.; Isakson, P. C. Pharmacological analysis of cyclooxygenase-1 in inflammation. *Proc. Natl. Acad. Sci. U. S. A.* **1998**, *95*, 13313–13318.

(34) Laufer, S. A.; Augustin, J.; Dannhardt, G.; Kiefer, W. 6,7-Diaryldihydropyrrolizin-5-yl)acetic acids, a novel class of potent dual inhibitors of both cyclooxygenase and 5-lipoxygenase. *J. Med. Chem.* **1994**, *37*, 1894–1897.

(35) Lamberth, C.; Dumeunier, R.; Trah, S.; Wendeborn, S.; Godwin, J.; Schneiter, P.; Corran, A. Synthesis and fungicidal activity of tubulin polymerisation promoters. Part 3: imidazoles. *Bioorg. Med. Chem.* **2013**, *21*, 127–134.

(36) Van Leusen, A. M.; Wildeman, J.; Oldenziel, O. H. Chemistry of sulfonylmethyl isocyanides. 12. Base-induced cycloaddition of sulfonylmethyl isocyanides to carbon,nitrogen double bonds. Synthesis of 1,5-disubstituted and 1,4,5-trisubstituted imidazoles from aldimines and imido-yl chlorides. *J. Org. Chem.* **1977**, *42*, 1153–1159.

(37) Lou, K.; Yao, Y.; Hoye, A. T.; James, M. J.; Cornec, A. S.; Hyde, E.; Gay, B.; Lee, V. M.; Trojanowski, J. Q.; Smith, A. B., III; Brunden, K. R.; Ballatore, C. Brain-penetrant, orally bioavailable microtubule-stabilizing small molecules are potential candidate therapeutics for Alzheimer's disease and related tauopathies. *J. Med. Chem.* **2014**, *57*, 6116–6127.

(38) Fukushima, N.; Furuta, D.; Hidaka, Y.; Moriyama, R.; Tsujiuchi, T. Post-translational modifications of tubulin in the nervous system. *J. Neurochem.* **2009**, *109*, 683–693.

(39) Kovalevich, J.; Cornec, A. S.; Yao, Y.; James, M.; Crowe, A.; Lee, V. M.; Trojanowski, J. Q.; Smith, A. B., III; Ballatore, C.; Brunden, K. R. Characterization of brain-penetrant pyrimidine-containing molecules with differential microtubule-stabilizing activities developed as potential therapeutic agents for Alzheimer's disease and related tauopathies. *J. Pharmacol. Exp. Ther.* **2016**, *357*, 432–450.

(40) Tries, S.; Neupert, W.; Laufer, S. The mechanism of action of the new antiinflammatory compound ML3000: inhibition of 5-LOX and COX-1/2. *Inflammation Res.* **2002**, *51*, 135–143.

(41) Meirer, K.; Steinhilber, D.; Proschak, E. Inhibitors of the arachidonic acid cascade: interfering with multiple pathways. *Basic Clin. Pharmacol. Toxicol.* **2014**, *114*, 83–91.

(42) Gillard, J. W.; Morton, H. E.; Fortin, R.; Guindon, Y. Preparation and formulation of 3-hetero-substituted-N-benzyl-indoles as inhibitors of leukotriene biosynthesis. EP275667A1, 1988.

(43) Schneider, L. S.; Mangialasche, F.; Andreasen, N.; Feldman, H.; Giacobini, E.; Jones, R.; Mantua, V.; Mecocci, P.; Pani, L.; Winblad, B.; Kivipelto, M. Clinical trials and late-stage drug development for Alzheimer's disease: an appraisal from 1984 to 2014. *J. Intern. Med.* **2014**, *275*, 251–283.

(44) Choi, S. H.; Aid, S.; Caracciolo, L.; Minami, S. S.; Niikura, T.; Matsuo, Y.; Turner, R. S.; Mattson, M. P.; Bosetti, F. Cyclooxygenase-1 inhibition reduces amyloid pathology and improves memory deficits in a mouse model of Alzheimer's disease. *J. Neurochem.* **2013**, *124*, 59–68.

(45) McGeer, P. L.; McGeer, E. G. NSAIDs and Alzheimer disease: epidemiological, animal model and clinical studies. *Neurobiol. Aging* **2007**, *28*, 639–647.

(46) Yan, Q.; Zhang, J.; Liu, H.; Babu-Khan, S.; Vassar, R.; Biere, A. L.; Citron, M.; Landreth, G. Anti-inflammatory drug therapy alters beta-amyloid processing and deposition in an animal model of Alzheimer's disease. *J. Neurosci.* **2003**, *23*, 7504–7509.

(47) Lim, G. P.; Yang, F.; Chu, T.; Chen, P.; Beech, W.; Teter, B.; Tran, T.; Ubeda, O.; Ashe, K. H.; Frautschy, S. A.; Cole, G. M.

Ibuprofen suppresses plaque pathology and inflammation in a mouse model for Alzheimer's disease. *J. Neurosci.* **2000**, *20*, 5709–5714.

(48) Lim, G. P.; Yang, F.; Chu, T.; Gahtan, E.; Ubeda, O.; Beech, W.; Overmier, J. B.; Hsiao-Ashec, K.; Frautschy, S. A.; Cole, G. M. Ibuprofen effects on Alzheimer pathology and open field activity in APPsw transgenic mice. *Neurobiol. Aging* **2001**, *22*, 983–991.

(49) Szekely, C. A.; Thorne, J. E.; Zandi, P. P.; Ek, M.; Messias, E.; Breitner, J. C.; Goodman, S. N. Nonsteroidal anti-inflammatory drugs for the prevention of Alzheimer's disease: a systematic review. *Neuroepidemiology* **2004**, *23*, 159–169.

(50) Martin, B. K.; Szekely, C.; Brandt, J.; Piantadosi, S.; Breitner, J. C.; Craft, S.; Evans, D.; Green, R.; Mullan, M. Cognitive function over time in the Alzheimer's Disease Anti-inflammatory Prevention Trial (ADAPT): results of a randomized, controlled trial of naproxen and celecoxib. *Arch. Neurol.* **2008**, *65*, 896–905.

(51) Breitner, J. C.; Baker, L. D.; Montine, T. J.; Meinert, C. L.; Lyketsos, C. G.; Ashe, K. H.; Brandt, J.; Craft, S.; Evans, D. E.; Green, R. C.; Ismail, M. S.; Martin, B. K.; Mullan, M. J.; Sabbagh, M.; Tariot, P. N. Extended results of the Alzheimer's disease anti-inflammatory prevention trial. *Alzheimer's Dementia* **2011**, *7*, 402–411.

(52) Leoutsakos, J. M.; Muthen, B. O.; Breitner, J. C.; Lyketsos, C. G. Effects of non-steroidal anti-inflammatory drug treatments on cognitive decline vary by phase of pre-clinical Alzheimer disease: findings from the randomized controlled Alzheimer's Disease Anti-inflammatory Prevention Trial. *Int. J. Geriatr. Psychiatry* **2012**, *27*, 364–374.

(53) Maxis, K.; Delalandre, A.; Martel-Pelletier, J.; Pelletier, J. P.; Duval, N.; Lajeunesse, D. The shunt from the cyclooxygenase to lipoxygenase pathway in human osteoarthritic subchondral osteoblasts is linked with a variable expression of the 5-lipoxygenase-activating protein. *Arthritis Res. Ther.* **2006**, *8*, R181.

(54) Varghese, M.; Lockey, R. F. Aspirin-exacerbated asthma. *Allergy, Asthma, Clin. Immunol.* **2008**, *4*, 75–83.

(55) Duffield-Lillico, A. J.; Boyle, J. O.; Zhou, X. K.; Ghosh, A.; Butala, G. S.; Subbaramaiah, K.; Newman, R. A.; Morrow, J. D.; Milne, G. L.; Dannenberg, A. J. Levels of prostaglandin E metabolite and leukotriene E(4) are increased in the urine of smokers: evidence that celecoxib shunts arachidonic acid into the 5-lipoxygenase pathway. *Cancer Prev. Res.* **2009**, *2*, 322–329.

(56) Perry, D.; Sperling, R.; Katz, R.; Berry, D.; Dilts, D.; Hanna, D.; Salloway, S.; Trojanowski, J. Q.; Bountra, C.; Krams, M.; Luthman, J.; Potkin, S.; Gribkoff, V.; Temple, R.; Wang, Y.; Carrillo, M. C.; Stephenson, D.; Snyder, H.; Liu, E.; Ware, T.; McKew, J.; Fields, F. O.; Bain, L. J.; Bens, C. Building a roadmap for developing combination therapies for Alzheimer's disease. *Expert Rev. Neurother.* **2015**, *15*, 327–333.

(57) Mariano, M.; Schmitt, C.; Miralinaghi, P.; Catto, M.; Hartmann, R. W.; Carotti, A.; Engel, M. First selective dual inhibitors of tau phosphorylation and Beta-amyloid aggregation, two major pathogenic mechanisms in Alzheimer's disease. *ACS Chem. Neurosci.* **2014**, *5*, 1198–202.

(58) Zhang, N.; Ayril-Kaloustian, S.; Nguyen, T.; Afragola, J.; Hernandez, R.; Lucas, J.; Gibbons, J.; Beyer, C. Synthesis and SAR of [1,2,4]triazolo[1,5-a]pyrimidines, a class of anticancer agents with a unique mechanism of tubulin inhibition. *J. Med. Chem.* **2007**, *50*, 319–327.

(59) Brunden, K. R.; Trojanowski, J. Q.; Smith, A. B., III; Lee, V. M.; Ballatore, C. Microtubule-stabilizing agents as potential therapeutics for neurodegenerative disease. *Bioorg. Med. Chem.* **2014**, *22*, 5040–5049.

(60) Zhang, B.; Maiti, A.; Shively, S.; Lakhani, F.; McDonald-Jones, G.; Bruce, J.; Lee, E. B.; Xie, S. X.; Joyce, S.; Li, C.; Toleikis, P. M.; Lee, V. M. Y.; Trojanowski, J. Q. Microtubule-binding drugs offset tau sequestration by stabilizing microtubules and reversing fast axonal transport deficits in a tauopathy model. *Proc. Natl. Acad. Sci. U. S. A.* **2005**, *102*, 227–231.